THESIS FOR THE DEGREE OF LICENTIATE OF ENGINEERING

Isochrone-Based Voyage Optimization Methods to Increase Shipping Energy Efficiency

YUHAN CHEN

Department of Mechanics and Maritime Sciences
CHALMERS UNIVERSITY OF TECHNOLOGY
Gothenburg, Sweden 2024

Isochrone-Based Voyage Optimization Methods to Increase Shipping Energy Efficiency

YUHAN CHEN

Report No 2024:06

Chalmers University of Technology
Department of Mechanics and Maritime Sciences
Division of Marine Technology
SE-412 96, Gothenburg
Sweden
Telephone: + 46 (0)31-772 1000

Printed by Chalmers Reproservice
Gothenburg, Sweden 2024

Isochrone-Based Voyage Optimization Methods to Increase Shipping Energy Efficiency

YUHAN CHEN
Chalmers University of Technology
Department of Mechanics and Maritime Sciences
Division of Marine Technology

Abstract

The International Maritime Organization (IMO) mandates improved energy efficiency in shipping, with voyage optimization systems being a key measure. The systems rely on ship models to estimate energy costs, and optimization algorithms to find the optimal route. However, models using various modelling techniques have been arbitrarily applied for voyage optimization in existing research. Their effectiveness needs systematic evaluation. Optimization algorithms plan the optimal voyage before departure, but uncertainties en route, such as weather and market changes, also require the algorithms to update voyages in real time to ensure optimal operations.

The main objectives of this thesis are to 1) investigate the sensitivity of various ship energy cost models in evaluating energy efficiency for ship voyage optimization, 2) develop strategies to improve the Isochrone voyage optimization algorithm, which is well-known for its computational efficiency, 3) propose an Isochrone-based predictive optimization algorithm for real-time ship voyage planning and execution for energy efficiency shipping.

Firstly, five ship models are integrated into a voyage optimization algorithm to identify their impacts on optimization. It is found that machine learning models present better reliability than theoretical models in diverse sailing environments, and considering specific fuel oil consumption (*SFOC*) variation in actual operation is essential to estimate accurate fuel costs. Secondly, five strategies are proposed to improve the traditional Isochrone algorithm. It is found that one proposed strategy, named 'Isochrone A*', can effectively resolve its drawbacks, such as unrealistic routes and locally optimized results. Meanwhile, it provides the most fuel savings. Based on these two findings, an Isochrone-based predictive optimization (IPO) method is finally proposed, with enhanced performance while remaining computational efficient. The proposed method has been validated using six case study voyages with full-scale measurements, and compared with four voyage optimization algorithms. It is found that, the proposed IPO method demonstrates smoother voyages with on-time arrivals and an average fuel reduction of 5% across diverse sailing conditions. Its runtime of around 40 seconds is also suitable for real-time usages.

Keywords: energy efficiency, estimated time of arrival, Isochrone algorithm, voyage optimization.

Preface

This thesis presents research work performed from March 2022 to August 2024, at the Division of Marine Technology, Department of Mechanics and Maritime Sciences, Chalmers University of Technology, Sweden. Financial support was provided by the AUTOBarge, the European Union's Framework Program for Research and Innovation Horizon 2020 under Grant 955768, the Swedish Vinnova Project under Grant 2021-02768, and the Lighthouse Sustainable Shipping Program.

It has been two and a half years since I started my PhD journey. Taking this opportunity, I would like to first express my sincere appreciation for my main supervisor, Professor Wengang Mao. Thank you for giving me the opportunity to become a PhD student, and for all the valuable and insightful supervision, suggestions, discussions and support you have provided since I started. Research was the hardest at the beginning, but you have provided enlightening guidance not only on the specific research topic, but also on conducting research in general.

I would also like to extend my gratitude to my examiner and co-supervisor, Professor Jonas Ringsberg. Thank you very much for all your warm support, help, and guidance as my academic supervisor and manager. In addition, thanks to your tireless work, our division has always been an enjoyable workplace. Furthermore, my special thanks go to all my friends and colleagues in our division, Chengqian (even part of this thesis template is owing to his contribution) and his wife Xue, Xiao, and Chi; also to my great friends in China, Ge, Rui and her little daughter Beike.

Last but not least, special thanks to my partner Wenting and our little cat Potato, for always being my strongest support. I used to not fully understand the idea that without someone, I could never achieve the goals as people ultimately have to accomplish their tasks on their own, but now I changed my mind. It is thanks to you that I have been able to remain calm, rational, and prepared to face all the challenges during this time. Thanks also to my family and parents for their understanding and unwavering support, even while I was away for important family matters, and for never blaming me.

The final part is dedicated to my grandfather, who left me last summer, June 2023. I planned many times how I should memorize you here, but still, I do not know how. I still cannot. I am sorry for holding such a false hope and think you will recover and wait for my return, as many times before. I do hope you will have a wonderful new life, without any disease and suffering any more. It must be a good life.

Yuhan Chen
Gothenburg, August 2024

Contents

List of appended papers

Paper I **Chen, Y.**, Mao, W., 2024. Sensitivity of ship voyage optimizations to various energy cost models. *Proceedings of the ASME 2024 43rd International Conference on Ocean, Offshore and Arctic Engineering (OMAE2024)*: 9-14 June 2024, Singapore. Paper no. OMAE2024-127986. DOI: 10.1115/OMAE2024-127986.

Paper II **Chen, Y.**, Tian, W., Mao, W., 2024. Strategies to improve the Isochrone algorithm for ship voyage optimization. *Ships and Offshore Structures*. pp.1-13. DOI: 10.1080/17445302.2024.2329011.

Paper III **Chen, Y.**, Mao, W., 2024. An Isochrone-Based Predictive Optimization for Efficient Ship Voyage Planning and Execution. *IEEE Transactions on Intelligent Transportation Systems*. DOI: 10.1109/TITS.2024.3416349.

List of other relevant papers by the author

Paper A **Chen, Y.**, Mao, W., Zhang, C., 2023. Different strategies to improve Isochrone voyage optimization algorithm. In *Advances in the Analysis and Design of Marine Structures* (pp. 53-61). CRC Press. DOI:10.1201/9781003399759.

Paper B Guo, Y., Wang, Y., **Chen, Y.**, Wu L., Mao W., 2024. Learning-based Pareto-optimum routing of ships incorporating uncertain met-ocean forecasts. Under review in *Transportation Research Part E: Logistics and Transportation Review.*

Nomenclature

Greek notations

ΔD	Parameter controlling the searching width of each local subsector [-]
ΔV	Reduction of speed for ship in the water [m/s]
Δt	Sailing time between two adjacent time stages [h]
$\Delta\theta$	Heading increment in angles, between two neighboring sub-routes from each of the current 'optimal' waypoints at each time stage [°]
η	Propulsion efficiency coefficient [-]
θ_c	Speed direction of ocean current [°]
θ_w	Speed direction of wind [°]
θ_{ref}	Reference course at each waypoint for sailing to the next time stage [°]

Latin notations

$C_{inv(ref)}$	Arrival course of GC_{ref} at the destination waypoint $\boldsymbol{P_f}$ [°]
C_{ref}	Initial course of GC_{ref} at the departure waypoint $\boldsymbol{P_0}$ [°]
d_i	Current distance to $\boldsymbol{P_0}$ at the i^{th} time stage [km]
d_{iS}	Current distance to $\boldsymbol{P_f}$ at the i^{th} time stage [km]
d_{total}	Total distance from $\boldsymbol{P_0}$ to $\boldsymbol{P_f}$ [km]
D	Geographical distance between $\boldsymbol{P_0}$ and $\boldsymbol{P_f}$ [km]
F_c	Overall fuel consumption [ton]
GC_{ref}	Great circle reference route between $\boldsymbol{P_0}$ and $\boldsymbol{P_f}$ [-]
H_s	Significant wave height [m]
m	$(2m+1)$ represents the number of successor waypoints for each waypoint at the current stage [-]
$\boldsymbol{P_0}$	Departure waypoint vector of a voyage [-]
$\boldsymbol{P_f}$	Destination waypoint vector of a voyage [-]
P_s	Engine propulsion power [kW]
r	$2r$ indicates the number of subsectors [-]
R_{Calm}	Calm water resistance of a ship [kN]
R_{Wave}	Wave resistances of a ship [kN]
R_{Wind}	Added wind resistances of a ship [kN]
R_{Total}	Total resistance of a ship [kN]
$SFOC$	Specific fuel oil consumption [g/kWh]
T_0	Departure time at $\boldsymbol{P_0}$ [h]
T_i	Time at the i^{th} time stage [h]
T_f	Arrival time at $\boldsymbol{P_f}$ [h]
T_z	Wave period [Hz]
V	Ship's speed through water [m/s]
V_c	Speed of ocean current [m/s]

V_g	Ship's speed over ground [m/s]
V_s	Pre-determined reference speed of ship [m/s]

Abbreviations

2D	Two-dimensional
3D	Three-dimensional
ACO	Ant colony optimization
AI	Artificial intelligence
ANN	Artificial neural network
BBM	Black-box model
CFD	Computational fluid dynamics
EA	Evolutional algorithm
ETA	Estimated time of arrival [h]
EU	European Union
GA	Genetic algorithm
GAM	Generalized additive model
GBM	Grey-box model
GC	Great circle route
GHG	Greenhouse gas
IMO	International Maritime Organization
IPO	Isochrone-based predictive optimization
JIT	Just in time
LR	Linear regression
ML	Machine learning
PR	Polynomial regression
PSO	Particle swarm optimization
SVR	Support vector regression
WBM	White-box model
XGBoost	Extreme gradient boosting

1 Introduction

This chapter first presents an overview of the background and literature reviews for the research conducted in this thesis. Further, the motivations and objectives are illustrated, along with the limitations in work scope.

1.1 Background

Over the past 20 years, seaborne trade has also exhibited a significant upward trend, as shown in Figure 1.1. It plays a vital role in global trade (Wu et al., 2021; Yan et al., 2022), contributing approximately 80% of the global economy (UNCTAD, 2021). Considering this vast scale, even a modest average fuel savings of 1% can lead to a reduction of about 8 million metric tons of CO_2 annually. The International Maritime Organization (IMO) has strengthened its greenhouse gas (GHG) strategy, aiming for a 20% reduction in emissions by 2030 and achieving net-zero emissions by 2050 (IMO, 2020a). Thus, the maritime community is actively advocating for the development and implementation of various measures to enhance shipping energy efficiency, and reduce fuel consumption and emissions. Meanwhile, as fuel costs can constitute a significant portion of overall operational expenses (Fan et al., 2022; Zhen et al., 2020), maintaining cost-efficiency in shipping also requires a strong focus on energy efficiency, particularly for shipping companies.

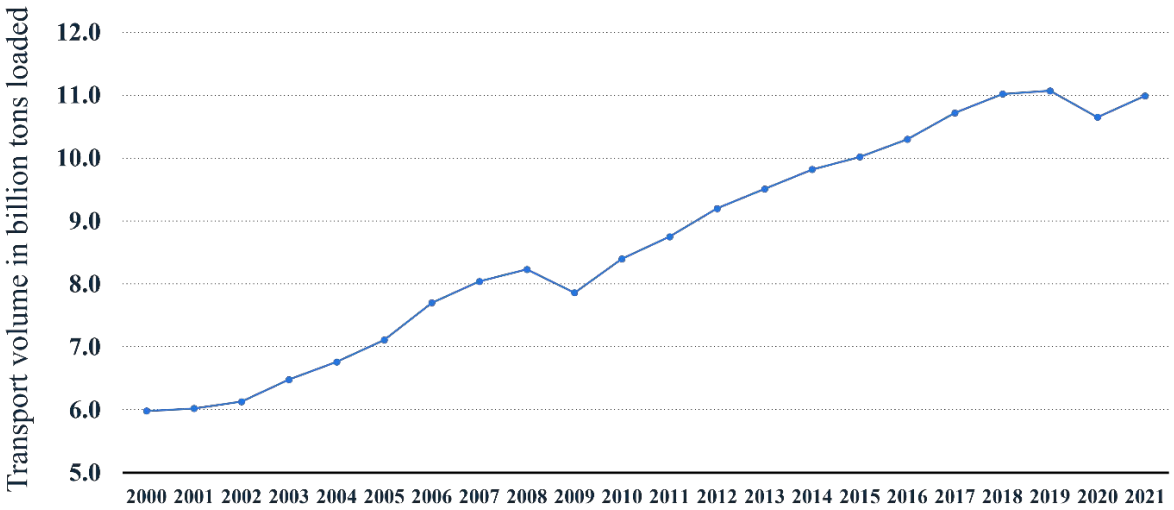

Figure 1.1: Transport volume of seaborne trade from 2000 to 2021 (UNCTAD, 2021).

Improving shipping energy efficiency has long been a major focus in both industry and academia. Ship voyage optimization is recognized as an efficient approach and is increasingly valued, because of its ability to ensure the quality of ship operations, such as safety and accurate travel times, while also advancing towards energy efficiency goals (Poulsen et al., 2022; Zis et al., 2020).

Zis et al. (2020) considered voyage optimization as a decision-making process, aimed at selecting the optimal route for a given voyage, with a known origin and destination port. The optimality of the selected route depends on the defined objectives. For seagoing vessels, environmental conditions influence the ship's performance most significantly, thereby making their optimization a weather-dependent process. Thus, voyage optimization for ocean crossings is mainly studied as an interdisciplinary problem of weather routing, attracting attention from various fields including ocean engineering, data science, and maritime economics.

Figure 1.2 illustrates a voyage optimization system with common components for seagoing vessels to achieve energy-efficient sailings. The energy efficiency can be evaluated by various specific optimization objectives, such as minimum fuel, power consumption, and emission, etc. (Lee et al., 2023; Poulsen et al., 2022; Wen et al., 2023). The constraints for voyage optimization include, for example, land avoidance, no-go zones, traffic separation scheme, etc. Based on these constraints, a waypoint grid is generated to outline the feasible sailing region. At each waypoint in the grid, the local sailing environmental conditions can be characterized by several key factors, such as the encountered wind, waves, and currents. In addition, for each specific sea state, the ship performance model estimates the corresponding energy consumption for sailings. This information of energy consumption provided by ship models for a specific situation will be used by cost function, to e.g., calculate the overall cost and identify the global optimum, thereby making the ship model an essential part inside the cost function. Finally, central to the system is the optimization algorithm, which handles the decision-making process.

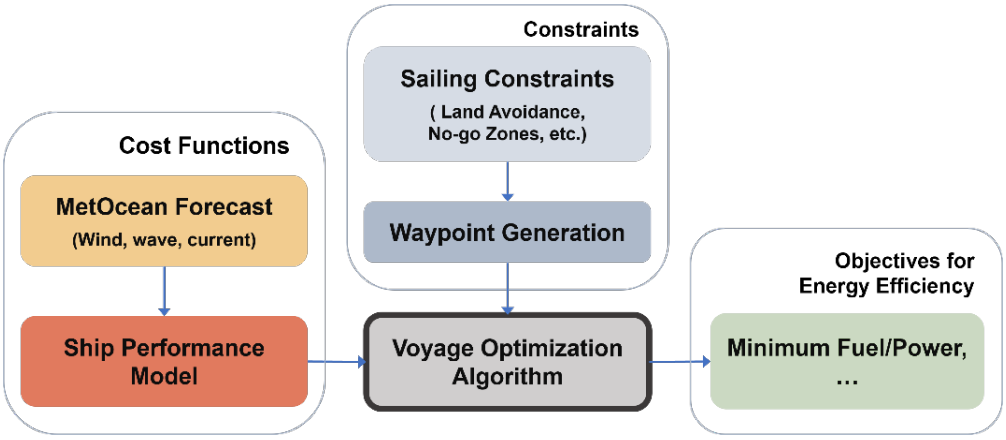

Figure 1.2: Overview of a voyage optimization system with objectives for energy efficiency.

Energy efficiency in the existing literature is defined in various ways, such as minimum fuel or power consumptions (Poulsen et al., 2022; Wang et al., 2021; Wen et al., 2023). Based on these specific definitions, ship performance models are formulated differently. As a result, different ship performance models may lead to varying results in optimization algorithms, and have different applications in voyage optimization, depending on the sailing conditions. Meanwhile, various techniques have been developed for performance modeling related to both power and fuel, e.g., empirical, physical,

and data-driven models. All these methods have been utilized in voyage optimization, but each has its strengths and weaknesses, which can lead to different outcomes. Variations in definitions of energy efficiency objectives, as well as modeling techniques may introduce uncertainties that impact the optimization process. Therefore, an investigation of the sensitivity and uncertainty of using different ship models is first required to ensure a reliable model is used in voyage optimization. That is, the model can accurately account for real-world complexities and uncertainties, ensuring that the applications of results from optimization algorithm remain consistent in practice.

Furthermore, to optimize an ocean-crossing voyage, the waypoint grid must cover a sufficiently large area around the route for effective search, which may require a vast number of waypoints to estimate the associated sailing costs. The computational requirements for such a voyage optimization system can easily exceed a computer's capacity. Consequently, optimization algorithms play a crucial role in determining the effectiveness of optimization and computational efforts.

Voyage optimization is generally applied in two separate stages: planning and execution (Poulsen et al., 2022). Voyage planning typically occurs prior to departure, relying on reliable weather forecasts. However, weather forecasts become highly uncertain beyond two or three days (European Centre for Medium-Range Weather Forecasts) while ocean-crossing voyages last much longer. This consequently necessitates updating the voyage to adapt to dynamic environmental conditions. Many algorithms output recommended speeds in the optimization results; however, a ship can rarely follow these exact speeds since seafarers often navigate a ship by setting the propulsion power or engine speed (RPM), and dynamic sea conditions can lead to variable sailing speeds under the same engine settings (Wang et al., 2021). Additionally, voyage execution can also be affected by various uncertainties and dynamics, including commercial factors such as fluctuating freight and charter rates, fuel prices, and blocked routes (Bai et al., 2022). These factors may compel ships to alter their original routes, estimated time of arrival (ETA), or destination ports while the ship is en route (Gao & Sun, 2023). The effectiveness of optimization algorithms in performing voyage optimization is vital for facilitating real-time adjustments during the voyage and managing weather conditions, commercial changes, and other operational uncertainties. Consequently, computationally efficient algorithms and simple ship navigation control configurations, like the two-dimensional (2D) Isochrone method, remain widely used due to their practicality.

The practical application of Isochrone methods has demonstrated their computational efficiency over the years (Hagiwara, 1989; Lin et al., 2013). As they are originally designed to plan routes that ensure arrival at a pre-specified time, these methods can support the just-in-time (JIT) arrival strategy advocated by the IMO. JIT approaches, which emphasize adhering strictly to planned schedules, are crucial in the industrial sector for enhancing efficiency and cost-effectiveness. They help reduce fuel consumption by avoiding excessive speeds, ensure timely operations, and minimize waiting times at ports (IMO, 2020b). Thus, the advantages of Isochrone optimization algorithms are that they firstly can generate optimal routes swiftly and adapt to changes, whether following the original plan or

accommodating flexible destination ports and ETAs. Secondly, they align well with the principles of JIT, achieving punctuality and operational efficiency. However, notable drawbacks of Isochrone algorithms are still evident, such as irregular turns and limited optimization capabilities. Therefore, improvements are necessary to address these limitations while maintaining its advantages such as computational efficiency.

1.2 Literature review

1.2.1 Terminology and definitions

As mentioned, ship voyage optimization is a widely studied and interdisciplinary field that incorporates research from various disciplines. Algorithms employed in voyage optimization have been extensively developed in many fields other than the maritime sector such as mathematics, computer science, and robotics, etc. These algorithms play a crucial role in enhancing the efficiency and effectiveness of optimization by providing reliable solutions for complex problems. However, the interdisciplinary nature of this research means that terminologies related to voyage optimization often vary, leading to ambiguity and confusion within both academia and industry. Furthermore, the interchangeable use of certain terms can result in misunderstandings and challenges in their application. Yu et al. (2021) presented a review which does not distinguish voyage optimization with ship routing/scheduling. Meanwhile, Zis et al. (2020) clarified that the 'ship routing/scheduling' is a completely different problem from the voyage optimization problem that discussed in this thesis.

This inconsistency highlights the need to present and standardize clear terminologies for effective communication and research regarding these algorithms. The following are common terms frequently used in voyage optimization research:

- **Voyage:** The berth-to-berth concept for voyages is applied according to European Parliament and of the Council (2015). That is, a voyage starts at the berth of one port of call, and ends at the berth of the next port of call.

- **Route:** A route is defined as a way or course taken from a starting point to a destination (Stevenson, 2010).

- **Routing:** The objective of a ships' routing is to "improve the safety of navigation in converging areas and in areas where the density of traffic is great or where freedom of movement of shipping is inhibited by restricted sea room, the existence of obstructions to navigation, limited depths or unfavorable meteorological conditions (IMO, 2003).

- **Weather routing:** Weather routing, by which ships are provided with 'optimum routes' to avoid bad weather, can enhance safety (IMO, 2003). Environmental routing and weather routing

are frequently used interchangeably, but the latter is a subset of the former. Both belong to the broader category of voyage optimization (Christiansen et al., 2007).

- **Voyage planning:** Voyage and passage planning includes four stages: 'appraisal', 'planning', 'execution', and 'monitoring'. At the 'planning' stage, a detailed voyage or passage plan should be prepared, covering the entire voyage or passage from berth to berth. This includes tasks such as plotting the intended route, tracking the voyage or passage, and, altering speed, course, and machinery status en route, etc. (IMO, 1999)

- **Voyage execution:** The voyage or passage should be executed in accordance with the plan, or any changes made thereto. Factors considered include, vessel navigation, ETA, meteorological conditions, weather routing information, and traffic conditions, etc. (IMO, 1999)

- **Ship scheduling:** The 'ship routing problem', or 'ship routing and scheduling problem', is a distribution problem at the tactical level in which a ship or a fleet of ships, has to serve several ports in order to pick up and deliver cargo, subject to various constraints such as ship capacity, and time windows (Zis et al., 2020).

- **Pathfinding:** Pathfinding is the algorithmic interpretation and implementation of attaining the shortest route(s) from a given source(s) to destination(s). It is a fundamental problem broadly studied in many fields such as artificial intelligence (AI), robotics, and computer science (Majumder & Majumder, 2021).

- **Path planning:** Finding a collision-free motion between an initial (start) and final configuration (goal) within a specified environment (Gasparetto et al., 2015).

In this thesis, voyage optimization refers to the weather routing problem as defined above. It is an optimization problem for a given voyage subject to different optimization objectives, e.g., energy efficiency. Thus, it is an operational-level challenge that focuses on how a single ship sails from a given departure port A to a designated destination port B. The route, along with other operational profiles such as speed and power, is optimized by considering environmental conditions. Voyage optimization is related to the broader problems of pathfinding and path planning. Consequently, many algorithms from these areas are applicable and constantly implemented.

1.2.2 Review of voyage optimization algorithms

In this thesis, voyage optimization focusses on seagoing vessels in open sea sailing. Thus, to achieve energy efficiency, optimization mainly takes into account weather and sea conditions (Simonsen et al., 2015; Zis et al., 2020). Examples of these objectives include minimum fuel consumption

(Gkerekos & Lazakis, 2020), lowest emissions (Yu et al., 2021; Zhao et al., 2019), or least structural damage (Mao et al., 2012), etc. In addition, a proper voyage needs to fulfil certain constraints, such as avoiding nearshore areas or land, the ship's sailing capability, and surrounding environmental conditions, based on metocean data and weather. Thus, the seagoing ship's voyage optimization relies heavily on weather data and specific ship characteristics. The weather information can include forecast data or predictions from a model, such as a model that predicts dynamic impacts on shipping, taking uncertainty into consideration (Vettor et al., 2021; Yuan et al., 2022). In addition to the weather model, a ship's behavior and response at sea can also be estimated and predicted by a ship performance model, for example, a statistical speed-power relationship (Lang & Mao, 2020) or a data-driven model (Lang et al., 2024), etc. These models analyze historical data, while a core component of the decision-making system is the voyage optimization algorithm, which searches for the optimized route within all the feasible solutions. The optimum route can be an output of a series of waypoints along the optimum course with a speed profile or, on a more operational level, settings such as heading angle, ship engine RPM and propulsion power (Wang et al., 2021; Wen et al., 2023).

Voyage optimization algorithms for seagoing vessels have been widely investigated throughout the years (Zis et al., 2020). Many well-established methods are available in the maritime transportation community, such as the Isochrone method, dynamic programming, Dijkstra and A* algorithms, and, more recently, AI and machine learning (ML) algorithms (Wang et al., 2021; Wang et al., 2019). They can be primarily categorized into 2D or three-dimensional (3D) methods, with a combination of requirements in real applications. Two-dimensional methods are more conventional, simplifying the problem into searching trajectories regarding only positions (waypoints with longitudes and latitudes), and assuming the other inputs such as speed and engine power, as fixed constants. Furthermore, they can be divided into static and dynamic grid-based methods. Static grid-based methods discretize the sailing area into small sections, within a certain range between departure and destination, and predefine a grid system based on these sections, e.g., dynamic programming method (Bellman, 1952) and, graph searching algorithms like the Dijkstra (Dijkstra, 1959) and A* algorithms (Hart et al., 1968), etc. Dynamic programming is based on Bellman's principle of optimality in which one problem is broken down into sub-tasks, and each of them is solved in sequence to obtain the optimal solution for the original problem. De Wit (1990) employed dynamic programming for ship sailing, separating voyage planning into a multi-stage process and validating its effectiveness. The Dijkstra algorithm is extended to derives the A* algorithm, by incorporating a heuristic component into the cost function. They have been applied in voyage optimization by, for example in recent years, Shin et al. (2020), Ari et al. (2013), Życzkowski et al. (2018), and Gkerekos and Lazakis (2020). These static grid-based algorithms are easy to construct into different forms, and suitable for both single and multiple objective optimization problems. However, the result as well as computation loads of static grid-based methods apparently relies heavily on the grid parameters, such as its resolution, the number of nodes, and the spatial extent it covers, etc., which makes the grid generation an influencing factor for the algorithm's performance, and therefore needs to be specifically taken care of for each voyage case.

Dynamic grid-based methods, on the other hand, conduct a search recursively, eliminating the need for a pre-defined grid. At each step, a subsequent node set is generated from the existing nodes, resulting in an iterative grid update. This process continues as paths are progressively developed until the destination is reached. A notable example of this approach is the Isochrone method, where an isochrone represents a line encompassing the farthest reachable waypoints, that a ship can reach following different directions within a certain period. This method was originally introduced by James (1957), however, the number of waypoints in this method can grow exponentially. Later adapted by Hagiwara (1989), he introduced an improved Isochrone method to resolve this problem. And this method has been used both manually and on computers for a long time because of its straightforward calculation. Another drawback of the original Isochrone method is the phenomenon known as the 'isochrone loop'. This irregular shape of an isochrone arises from the non-convex nature of a ship's performance (Roh, 2013; Wisniewski, 1991). As the number of isochrones increases, the isochrone loop effect propagates, resulting in impractical outcomes. Thus, Roh (2013) further improved the Isochrone algorithm. Klompstra et al. (1992) presented a similar approach as the isopone algorithm, which replace traveling time with an equivalent fuel consumption. Because of its relatively high computational efficiency, it has great value in practical applications. Moreover, since it continuously adapts and approaches the destination step by step, it can handle uncertainty and respond fast to the dynamic environment.

To allow for more complicated cases and achieve advanced planning, 3D algorithms have also been developed. One example is including time as an additional variable, such as Choi et al. (2023), Du et al. (2022) and Zaccone et al. (2018) who developed a 3D dynamic programming algorithm; Lin et al. (2013), Fang and Lin (2015), and Lin (2018) improved a 3D Isochrone method; Mannarini and Carelli (2019), Mannarini et al. (2023), Zyczkowski and Szlapczynski (2023) and Wang et al. (2019) proposed a 3D Dijkstra algorithm. Voyage optimization typically requires handling extensive data, adapting to dynamic changes, and making predictions under uncertainty, which renders the problem both large-scale and complex. Consequently, alongside the advancement of AI and ML techniques, more sophisticated methods have been developed in recent years, such as the utilization of the genetic algorithm (GA), evolutionary algorithm (EA), ant colony optimization (ACO), particle swarm optimization (PSO), and their variants. Alternative approaches can also implement ML algorithms, such as 3D EAs/GAs (Ma et al., 2021; Szlapczynska & Szlapczynski, 2019; Wang et al., 2021), and 3D ACO (Dong et al., 2021; Zhang et al., 2023). Zhang et al. (2022) proposed a 3D ACO specially for ice routing. Chen and Tan (2023), and Wang et al. (2022) utilized 3D PSO in decision-making, Gkerekos and Lazakis (2020), and Moradi et al. (2022) deployed 3D artificial neural network (ANN) to optimize fuel consumption of vessels. These algorithms consider speed/time variation along the voyage and, therefore have greater capabilities to achieve more competitive performance. However, a tradeoff exists between performance and efficiency, and because of its complexity, the computation loads also increase dramatically. Moreover, stochastic methods, such as GA, EA, ACO, and PSO, if given the same specific input, can generate different outputs each time they operate because of the

stochastic nature of these algorithms. A summary of advantages and disadvantages for these algorithms is presented in the following Table 1.1.

Table 1.1: Summary for advantage/disadvantage of optimization algorithm types commonly used in voyage optimization.

Type	2D		3D and multi-variables	
Description	Route with fixed speed		Route and speed (or power, RPM, etc.)	
Pros	1) Easy to apply, 2) Fast for computation		Superior optimization results	
Cons	Can lead to suboptimal and local optimization results		1) Slow computation, 2) Hard to apply results in real operation	
Method	Deterministic	Stochastic	Deterministic	Stochastic
Method Pros	Result can be found if exist	Stochastic nature helps to avoid local optimization	1) Result can be found if exist 2) Improved optimization capability by including more variations than 2D	1) Stochastic nature helps to avoid local optimization 2) More improved optimization capability, compared with deterministic methods
Method Cons	1) Discretized nature can lead to suboptimality 2) Optimization result improves by high grid resolution, but computation load also increases	1) Cannot guarantee an optimized result even one exists 2) Same inputs may not give same results	1) Heavier computation load by using extra variables than 2D 2) Challenging to apply results in real operation	1) Computation load increases heavily 2) Same inputs may not give same results 3) More challenging to apply results in real operation
Examples	(Hagiwara, 1989) (De Wit, 1990)	(Tsou, 2010) (Li et al., 2018) (Xue, 2022)	(Jeong et al., 2019) (Bahrami & Siadatmousavi, 2023)	(Ma et al., 2021) (Wang et al., 2021) (Ma et al., 2024)

1.2.3 Review of ship performance models

In a voyage optimization system, the cost function is also crucial, aiding the optimization algorithm in decision-making and identifying optimal solutions. Central to the cost function is the ship performance model. In this thesis, the ship model establishes the relationship between specific

environmental conditions (e.g., wind, wave and current) and the ship's energy consumptions of sailing under such environment (e.g., power or fuel). This energy consumption is then provided to the cost function, so that cost function can further utilize this information to assess e.g., the overall energy cost a solution, and therefore find the optimum.

Ship performance modeling has many approaches, e.g., empirical/semi-empirical methods, computational fluid dynamics (CFD), model testing, and ML. Among these, those suitable to be used in today's voyage optimization can be generally categorized into white-box models (WBMs), black-box models (BBMs), and grey-box models (GBMs) (Lang et al., 2024; Yan et al., 2024). WBMs rely on established shipping knowledge and physical principles, offering transparency, interpretability and good extrapolation ability. Examples include the models developed by Holtrop and Mennen (1982), Huang et al. (2018), Tillig and Ringsberg (2019), Mao and Rychlik (2017), and Lang and Mao (2020), etc. However, WBMs depend on prior knowledge, and accuracy is often constrained by assumptions and uncertainties inherent in the model.

In contrast, BBMs utilize extensive operational data and advanced ML techniques, such as ANNs (Bassam et al., 2023; Du et al., 2019), tree-based models (Soner et al., 2018; Yan et al., 2020), support vector machines (Ahlgren et al., 2019), and others (Lang et al., 2021, 2022) to predict ship performance. These models are praised for their superior fitting compared to WBMs, and generalization capabilities which do not require prior knowledge. However, their complexity and poor interpretability may hinder their acceptance among industry professionals. Additionally, they may have difficulty providing accurate predictions for unmeasured conditions, limiting their practical application in unpredictable dynamic sea environments.

To mitigate the limitations of WBMs and BBMs, researchers have also developed GBMs, which combine the theoretical foundations of WBMs with the data-driven insights of BBMs, such as those by Yang et al. (2019) and Wang et al. (2023). These approaches allow for more accurate and theoretically explainable predictions. GBMs have two forms: sequential, where WBMs and BBMs are applied in sequence, and parallel, where WBMs provide the theoretical framework and BBMs refine parameters based on empirical data (Yan et al., 2024).

These types of ship models have been used in voyage optimization, as demonstrated by Tzortzis and Sakalis (2021), Wang et al. (2020), and Li et al. (2020), who used WBMs; Beşikçi et al. (2016), Du et al. (2019), and Moradi et al. (2022) who used BBMs; and Coraddu et al. (2017) who used a GBM. However, as the behavior of different models varies under different conditions, different models may have varying impacts on optimization results. This variability in ship models thus motivates a sensitivity research of voyage optimization to ship models, which will be further introduced in the following Chapter 1.3.

1.3 Motivation and objectives

The various model types, WBM, BBM, and GBM, as discussed in Chapter 1.2.3, have strengths and weaknesses. WBMs are valued for their cost-effectiveness and ability to provide reliable and accurate predictions across various conditions. They are grounded in physical laws and offer good extrapolation beyond the measurement data. BBMs and GBMs hold promise for accurate modeling, but their effectiveness depends on the quality and quantity of measurement data. While WBMs may oversimplify complex phenomena, and BBMs and GBMs may struggle with unseen scenarios, all approaches carry their own uncertainties. Consequently, integrating different model approaches into cost function can lead to varying impacts on the optimization results, especially for voyages through diverse sea states.

Additionally, different performance models, such as those focusing on engine power or fuel consumption, may also vary in their application. These two factors—modeling techniques and energy costs related to power or fuel—have been employed differently in voyage optimization. This highlights the need to systematically evaluate the impact and sensitivity of these performance models for reliable models in decision-making of voyage optimization.

Advanced algorithms, which can manage a broader range and more flexible variations of control parameters in voyage optimization, can achieve superior optimization results. However, their significant computational demands and results containing constant navigation adjustments can make them impractical for real-world applications in the shipping industry. Ocean-crossing ships are typically large and require steady, minimal adjustments to sailing parameters such as speed, heading, and power. Frequent changes in sailing status necessitating continuous ship maneuvering can lead to increased fuel consumption, emissions, and navigation risks. As a result, they may struggle to implement the outputs from these complex algorithms (Simonsen et al., 2015). In addition, certain advanced meta-heuristic approaches, unlike deterministic methods such as Isochrone algorithms, do not always yield a solution even when possible.

According to a market survey by Simonsen et al. (2015), shipping companies expect the runtime of the voyage optimization algorithm to be within minutes, to be computational efficient enough for real-time adjustments and address uncertainties in execution. Thus, efficient and straightforward ship navigation configurations, such as the 2D Isochrone method, are widely used for their practicality. Initially designed to ensure accurate ETAs, the Isochrone methods align well with the industry's focus on JIT arrival. They quickly generate optimal routes, adapt to changes, and maintain punctuality, making them suitable for both fixed and flexible voyage plans. However, one notable drawback of the original Isochrone method is the occurrence of 'isochrone loops', which are irregular shapes due to the non-convexity of ship performance at sea (Roh, 2013). As the number of isochrones grows, these loops become more prevalent, resulting in impractical outcomes for real operation. Besides the shape of routes, Hagiwara's existing 2D Isochrone method (Hagiwara, 1989) also suffers from

significant issues with route convergence in its final stages, as shown in Figure 1.3. Many researchers have enhanced the Isochrone method by incorporating speed optimization or advanced ML algorithms, as presented in the literature review. However, they also increase complexity which influences its real-time capability.

Therefore, the main aim of this thesis is to propose an effective and efficient Isochrone-based optimization algorithm for energy efficient real-time voyage optimization. To achieve this main objective, there are three stepwise goals:

1) Identify the uncertainties of using different ship performance models in voyage optimization, and the sensitivity of the optimization to various ship performance models. Determine the reliable ship model to be used in voyage optimization, which can provide accurate performance predictions under diverse weather conditions.
2) Propose several strategies to improve the Isochrone method for energy efficiency real-time voyage optimization, and investigate which improvement is the most effective. Specifically, i) overcome the occurrence of irregular route shapes, ii) improve optimization capability to avoid local optimization. iii) maintain adequate computational efficiency, which stays within 1 minute.
3) Combing the above findings, propose the Isochrone-based algorithm that addresses voyage optimization problem to optimize energy efficiency and yield an accurate ETA for the given voyage under diverse sailing conditions. In addition, the routes are smooth for operation, and computation is efficient with runtime within 1 minute, allowing for voyage planning and real-time execution usage.

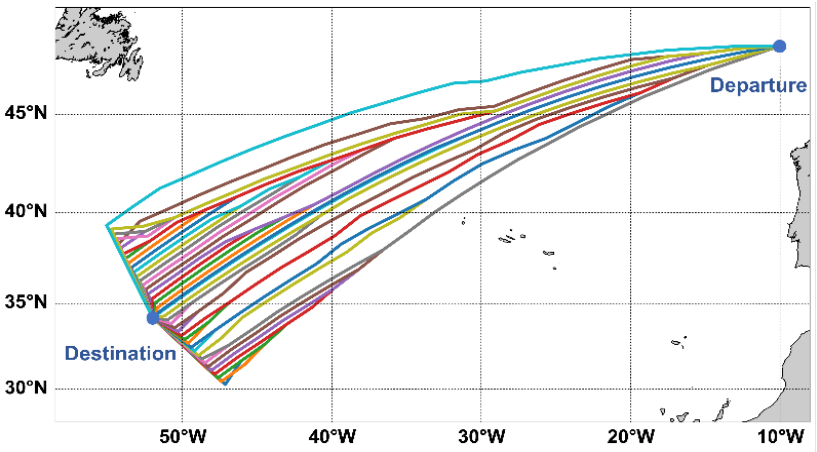

Figure 1.3: Example of an optimized route set where sharp turns are present near the destination from Hagiwara's method (Hagiwara, 1989).

1.4 Work scope and limitations

It should be noted that the following aspects are not covered in this thesis:

1) The proposed optimization algorithm addresses the voyage optimization problem for sea-going ships in open sea conditions, and does not account for ice-covered areas, short-sea shipping, or inland shipping. It assumes departure, destination port and ETA (associated with the service speed) have been determined and given as prerequisites before implementation.
2) The optimization algorithm requires a specific performance model for optimizing the voyage of a particular ship. Given such a ship model, the proposed optimization algorithm can be applied to optimize voyages for different types of ships and trades, extending beyond the specific ship used in case studies in this thesis.
3) Detailed ship safety and some other practical navigational considerations are not included. Comprehensive ship safety considerations such as models to describe safety margins, are beyond the scope of this study. These can be integrated in future practical implementations. Other critical aspects of ship navigation, including ship motions, collision avoidance, and maritime service fees, along with appropriate cost function models, can also be incorporated into the proposed method for multi-objective voyage optimization. However, these factors, along with detailed navigation planning considerations like traffic separation zones, keel clearance, and real-time navigation warnings from an ECDIS (electronic chart display and information system), are only partially addressed and will be explored in future research. Implementations involving bathymetric maps, tidal currents, and setting reference routes are not fully considered in this thesis.
4) The optimization algorithm assists seafarers in voyages planning and execution, based on the provided destination and ETA, and enhances energy efficiency for one voyage. To deploy optimization for voyage planning before departure, an example of the optimization process using Isochrone method by Hagiwara (1989) can be found in Figure 1.4. For voyage execution, as previously mentioned, this process involves constantly changing uncertainties. If any uncertainties, e.g. weather or commercial dynamics cause changes during the journey—such as a new port of call or revised ETA—the algorithm can swiftly adjust the voyage in real time. To address this, the method is proposed with emphasis on computational efficiency (i.e., runtime within 1 minute), which allows for update in real time, to optimize onboard based on emerging uncertainties. As the example shown in Figure 1.5, if deviations occur during execution, the current location can be updated as the new departure, with other updated inputs provided to restart the optimization algorithm, achieving effective optimization for execution and supporting seafarers in their decision-making.
5) Other factors during execution, such as traffic conditions, are also not included. As they require inputs such as real case studies and data collected from operation, method validations specifically focusing on voyage optimization for execution are not presented in this thesis. This will be explored in future research, which is elaborated in Chapter 6.

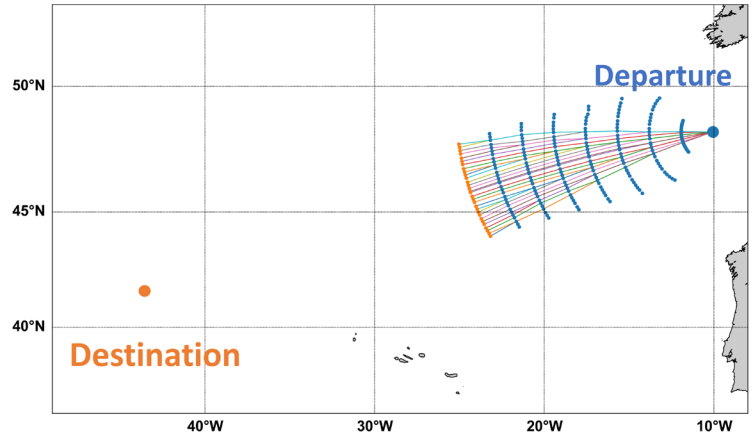

Figure 1.4: Example of the optimization process for voyage planning using Isochrone method.

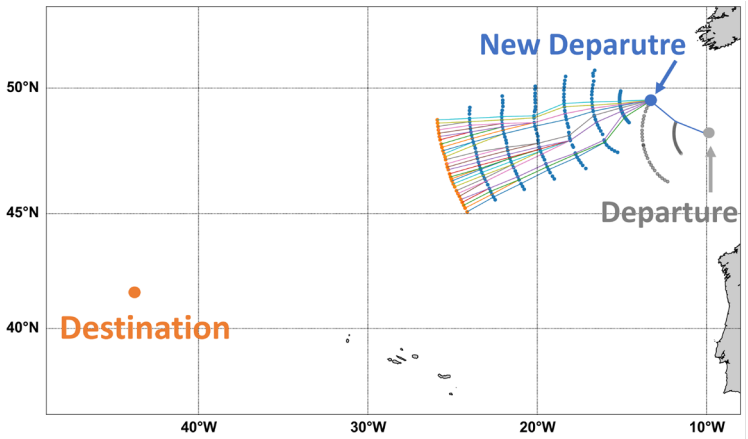

Figure 1.5: Example of the optimization process and restart of the algorithm for voyage execution using Isochrone method.

1.5 Outline of the thesis

The thesis is structured as follows: Chapter 2 illustrate ship energy performance models using various modeling techniques, and Chapter 3 presents the methods for developing a voyage optimization algorithm based on the Isochrone method. Chapter 4 summarizes the main findings and results from the appended publications. Chapter 5 presents the conclusions, and Chapter 6 discusses future work.

2 Ship performance models in voyage optimization

The ship model affects the accuracy of the optimization results in practical applications, as inaccuracies in the model can lead to discrepancies between the optimized results and their real-world implementation. Thus, the ship model is first investigated before improving the algorithm.

This chapter introduces the ship performance model used in voyage optimization along with different techniques for modelling. Firstly, an overview of the general voyage optimization problem is presented to emphasize the effect of the ship performance model, followed by an introduction to ship models and five modeling techniques adopted into investigation in the thesis.

2.1 An overview of voyage optimization problem

In a ship's voyage optimization process, as shown in Figure 2.1, the waypoint associated with the time T_i (i.e., the i^{th} time stage) should be first denoted:

$$\boldsymbol{P_i} = [x_i, y_i, T_i] \tag{2.1}$$

where the waypoint $\boldsymbol{P_i}$ includes the geographic location longitude x_i and latitude y_i. For such a location $\boldsymbol{P_i}$, we denote a ship's navigational conditions of the waypoint $\boldsymbol{P_i}$ to the next adjacent time stage $\boldsymbol{P_{i+1}}$ by $\boldsymbol{u_{i\rightarrow(i+1)}}$. Depending on methods, $\boldsymbol{u_{i\rightarrow(i+1)}}$ can include different factors, for example the sailing speed v and heading angles θ of the associated voyage leg.

$$\boldsymbol{u_{i\rightarrow(i+1)}} = [v, \theta\,] \tag{2.2}$$

A voyage consists of a series of waypoints, which is defined in Eq. (2.1), and the sub-routes connect each pair of adjacent waypoints is named 'voyage leg'. Let metocean environment encountered at the voyage leg associated with the waypoint $\boldsymbol{P_i}$, i.e., from $\boldsymbol{P_i}$ to its next adjacent waypoint $\boldsymbol{P_{i+1}}$, denoted by $\boldsymbol{w}(\boldsymbol{P_i})$, which includes parameters of wind, wave and current, as follows:

$$\boldsymbol{w}(\boldsymbol{P}) = [\,S\,(\omega\,|H_s, T_z), V_c, \theta_c, V_w, \theta_w\,] \tag{2.3}$$

where $S\,(\omega\,|H_s, T_z)$ representing the encountered waves consists of significant wave height H_s and wave period T_z. V_c, θ_c, V_w and θ_w include ocean current and wind information, in terms of speed and direction respectively.

Therefore, the control variables in the voyage optimization are the waypoints set $\boldsymbol{P}$ and ship navigational parameters $\boldsymbol{U}$, i.e., [$\boldsymbol{P}$, $\boldsymbol{U}$]. The task of a voyage optimization algorithm is to find a series of waypoints $\boldsymbol{P}$ associated with optimal navigational parameters $\boldsymbol{U}$ as follows,

$$\boldsymbol{P} = [\boldsymbol{P_1}, \boldsymbol{P_2}, \ldots \boldsymbol{P_{n-1}}, \boldsymbol{P_n}]$$
$$\boldsymbol{U} = [\boldsymbol{u_{1\to 2}}, \ldots, \boldsymbol{u_{(n-1)\to n}}] \tag{2.4}$$

where n denotes the last time stage, $\boldsymbol{P_n}$ denotes last waypoint before destination.

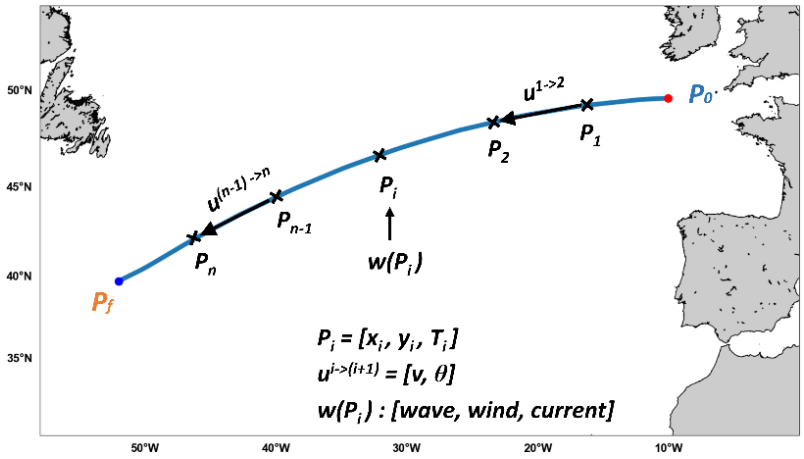

Figure 2.1: Example of a voyage with waypoints and other conditions.

The control variables [$\boldsymbol{P}$, $\boldsymbol{U}$] are determined by optimization algorithms to fulfil pre-defined optimization objectives, i.e., minimize the fuel consumption during the voyage while maintaining the ETA as follows:

$$C = \sum_{i=1}^{n} g\big(\boldsymbol{P}, \boldsymbol{U} \mid \boldsymbol{w}(\boldsymbol{P})\big) \tag{2.5}$$

where g ***(P, U| w)*** represents the instantaneous cost function for the optimization, i.e., the energy consumption of the specific voyage leg associated with the waypoint $\boldsymbol{P}$ with navigational conditions $\boldsymbol{U}$ under associated metocean conditions ***w(P)***.

The formulation of cost function can be method dependent on how to utilize and accumulate instantaneous energy cost of each voyage leg. And the ship model is responsible for predicting all the instantaneous energy cost. As presented in Table 2.1, the general input and output of a ship model are listed. Different methods are available to build such a model of ship performance in energy consumption, and they will be introduced and investigated in detail in the following subchapter 2.2.

Table 2.1: Summary of general inputs and outputs of a ship model.

Class	Description	Attributes
Input	Waypoint $\boldsymbol{P}$	$[x_i, y_i, T_i]$
	Navigational conditions $\boldsymbol{U}$	$[v, \theta\ ]$
	Metocean conditions $\boldsymbol{w}$ at $\boldsymbol{P}$	$[\ S\ (\omega\ \|H_s, T_z), V_c, \theta_c, V_w, \theta_w\ ]$
Output	Energy consumption	Various metrics, e.g., power or fuel

2.2 Ship energy performance model

For energy-efficient voyage optimization, the ship model estimates the energy consumption for each feasible route or sub-route based on sailing speeds and environmental conditions encountered. Therefore, the reliability of a ship's energy performance model significantly impacts the optimization results.

As outlined in the above voyage optimization procedures, the control variables [$\boldsymbol{P}$, $\boldsymbol{U}$] include the ship's speed, and the performance model presented in this section is used to predict the energy cost for the given $\boldsymbol{u} = [v, \theta]$ under the weather $\boldsymbol{w}$ at location $\boldsymbol{P}$. The general procedure follows procedures given in Figure 2.2, to develop a ship performance model and estimate the energy cost, e.g., power and fuel consumption.

Based on the ship's speed through water V, by combining the ship's characteristics and the encountered sea conditions, the total resistance R_{Total} is first obtained. The propulsion power P_s can then be calculated based on the effective power from the propeller against the resistance R_{Total}, engine configurations, and propeller efficiencies. Then, the fuel cost F_c is obtained based on P_s and specific fuel oil consumption ($SFOC$), representing the efficiency of the ship engine. The following relationships between F_c, P_s, and $SFOC$ generally applies:

$$F_c = P_s \times SFOC \tag{2.6}$$

To achieve the objective of minimum energy usage, the cost function can either be chosen to evaluate engine propulsion power, i.e., P_s, or the fuel consumption F_c. However, because of the hull-propulsion-engine coupling, the efficiencies of the engine, i.e. $SFOC$, are also significant for the final energy cost.

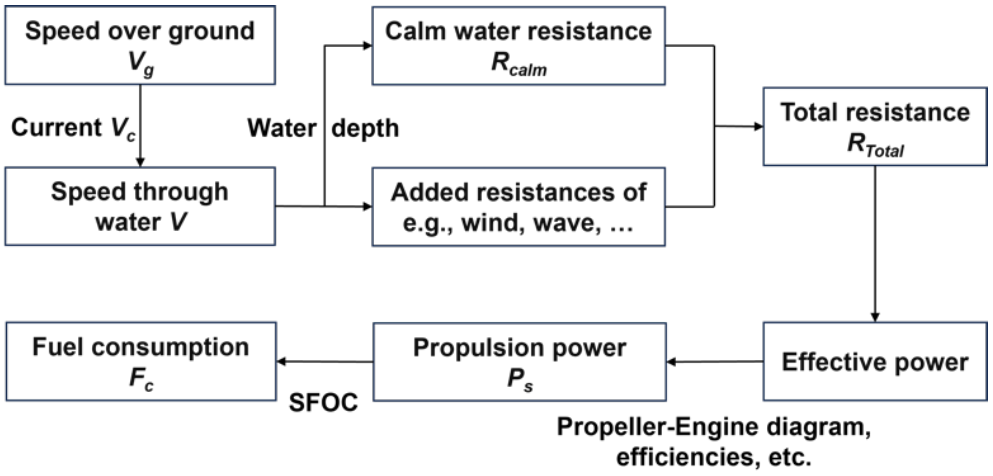

Figure 2.2: General ship energy consumption estimation process.

SFOC represents the efficiency of the engine, and its value varies under different speeds or propulsion power. In the industry, the data of *SFOC* are calibrated through a series of engine tests, and the curve of *SFOC* with respect to the propulsion power P_s is derived through data analyses. The theoretical *SFOC* curve indicates the average *SFOC* within the measured time interval, but discrepancies can remain between the measured *SFOC*, and the theoretical values from manufacturers. Figure 2.3 shows an example of *SFOC* measurement data collected for the engine of a chemical tanker ship, which will be used as a case study ship introduced in Chapter 4. The *SFOC* accuracy can therefore be improved through better modelling of *SFOC* under various operational conditions.

The concept of *SFOC* extends beyond fuel oil and applies to alternative fuels such as LNG (liquefied natural gas), methanol, and ammonia. The underlying principle remains the same, reflecting the engine's efficiency in converting fuel energy into useful work. Engines using these alternative fuels can possess different *SFOC* values, owing to differences in energy densities and combustion properties, but the estimation process is similar.

Thus, firstly, optimization based on power P_s may yield different results compared to using fuel F_c in the optimization process. Furthermore, they can both be modelled in various ways from exiting research, such as empirical (Lang & Mao, 2020, 2021) and sing more advanced ML approaches (Lang et al., 2022, 2024). Additionally, *SFOC* varies under actual operational conditions, also potentially causing discrepancies in fuel estimation and affecting voyage optimization. Further investigation is needed to understand how they influence voyage optimization.

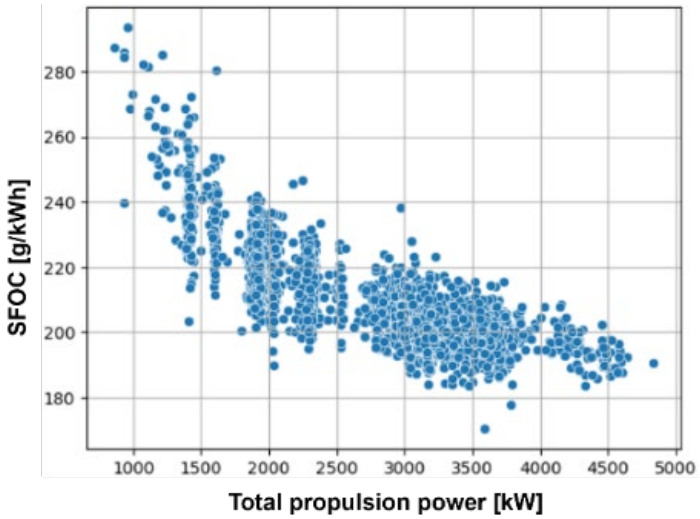

Figure 2.3: The measurement data of *SFOC* under different propulsion powers.

In this thesis, five models are formulated to estimate energy efficiency. Two metrics, i.e., fuel F_c and power P_s, are used to quantify energy cost or efficiency due to their common usage. They can both be modeled by various techniques, among which, the theoretical and data-driven modeling are two of the most widely used ones, as reviewed in Chapter 1.2.3. Thus, first for power consumption, a power WBM and a BBM are used. Further, theoretical and data-driven *SFOC* modeling are also

presented. These *SFOC* combining with power WBM and BBM respectively, it derives three fuel models, WBM, GBM, and BBM, as given in Table 2.2 and detailed in Figure 2.4.

Table 2.2: Performance models used in the cost function.

Category	Model	Speed-Power	*SFOC*
Power as cost	Theoretical power (WBM)	Theoretical	-
	ML power (BBM)	ML	-
Fuel as cost	Theoretical fuel (WBM)	Theoretical	Theoretical
	ML power + Theoretical *SFOC* (GBM)	ML	Theoretical
	ML fuel (BBM)	ML	ML

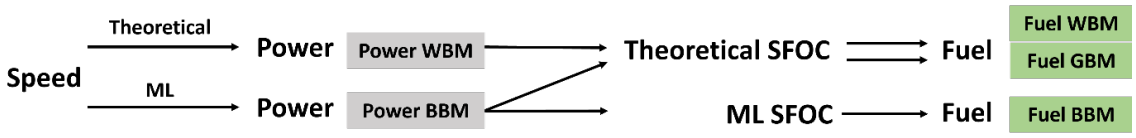

Figure 2.4: Performance models used in the cost function.

2.3 Different energy performance models for voyage optimization

In this chapter, five ship models are introduced in detail respectively, i.e., power WBM and BBM, and fuel WBM, GBM, and BBM.

Theoretical power model – power WBM

Since the propulsion power directly relates to the total work done by the engine, the first cost function aims to optimize the overall sailing cost by minimizing the propulsion power, i.e., it includes a speed-power relationship. In this part, the ship performance model is developed by a conventional theoretical approach as shown in Figure 2.2.

Ocean current affects the ship by correcting its speed over ground, into speed through water (Lang & Mao, 2020). Starting from the speed over ground V_g, we need to first determine the ship's speed through water V. According to ISO 15016 (Ships, 2015), the superposition principle is applied to derive V from V_g and the speed of ocean current V_c:

$$V = V_g + V_c \tag{2.7}$$

Then based on the encountered sea condition, and the ship's characteristics, the total resistance R_{Total} is derived from adding calm water resistance R_{Calm}, added wind resistances R_{Wind}, and wave resistance R_{Wave}:

$$R_{Total} = R_{Calm} + R_{Wind} + R_{Wave} \tag{2.8}$$

The above forces are calculated based on (Lang & Mao, 2020, 2021) in this part. The total resistance R_{Total} is counteracted by the effective power from the engine and propellers to propel the ship forward under the speed through water V. The effective power multiplied by some efficiencies equals the propulsion power P_s. This means that the propulsion power P_s is the effective power adjusted by efficiencies, derived as follows:

$$P_s = R_{Total} \times \eta \times V \tag{2.9}$$

where η is the overall efficiency coefficient calculated based on (Holtrop & Mennen, 1982). It includes relative rotative efficiency, hull efficiency, propeller open water efficiency, and engine shaft efficiency. Eventually, the theoretical $V - P_s$ relationship in Eq. (2.9) between the speed through water V to the propulsion power P_s is generally modelled as:

$$P_S = F_W(\boldsymbol{x}),\ \boldsymbol{x} = \{V\} \tag{2.10}$$

ML power model — power BBM

Recent research and industry advancements have led to the development of ML models. Many ML techniques have been applied to describe the speed-power relationship of ships in existing research. Lang et al. (2022) conducted a comparison study of ML techniques in ship performance modeling, to find the one that can build models with the least performance prediction discrepancy, i.e., the error between the model output and the real measurement data. Methods including linear and polynomial regressions (LRs and PRs), generalized additive models (GAMs), ANNs, support vector regressions (SVRs), and XGBoost (Extreme Gradient Boosting) were developed and compared (Lang et al., 2022). And the comparison result is in Figure 2.5, showing that the XGBoost technique demonstrates a discrepancy of no more than 3% in power prediction for around ten days of actual sailing. In contrast, other methods such as ANN, SVR, GAM, and statistical LR and PR, show discrepancies of around 20-30% between the model predictions and actual measurements.

Thus, this thesis develops a ML speed-power BBM following the workflow in Figure 2.6 using XGBoost technique. XGBoost is a powerful and advanced ML technique used for regression and classification problems (Chen & Guestrin, 2016). For model training, the output is the measured propulsion power P_s, while the input features include operational and environmental variables, detailed in Table 2.3. Those input features can be extracted from case study ship's characteristics, and measurements including ship operational data and metocean data from real sailings. The XGBoost model aims to establish the relationship $F_{ML}(\boldsymbol{x})$ between input $\boldsymbol{x}$ and P_s, as given in the following Eq. (2.11).

$$P_S = F_{ML}(\boldsymbol{x}),\ \boldsymbol{x} = \{V, T, Trim, HDG, H_S, T_Z, D_{wave}, U_{wind}, V_{wind}\} \quad (2.11)$$

Finally, the trained XGBoost model is integrated into the cost function of the voyage optimization algorithm, to evaluate propulsion power P_s for specific $\boldsymbol{x}$ associated with waypoints, and establish the minimized P_s for the given voyage.

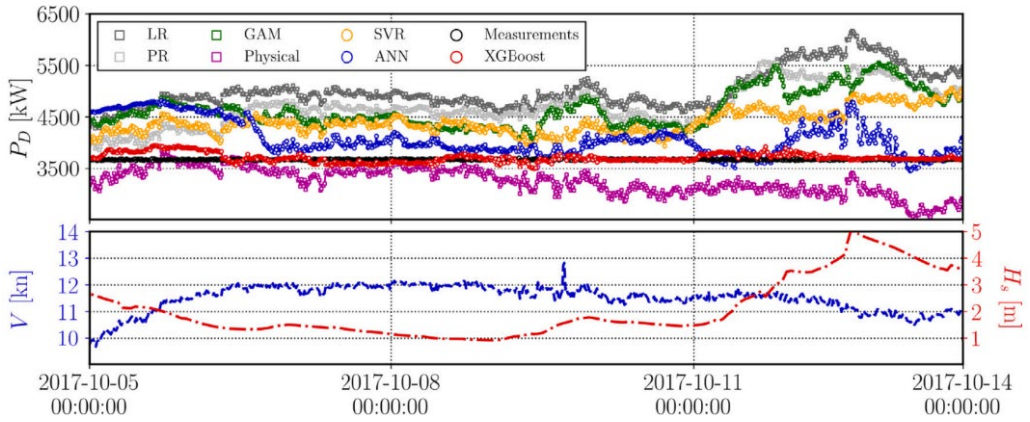

Figure 2.5: Comparison for a case study voyage in propulsion power prediction using different ML models (Lang et al., 2022).

Table 2.3: Attributes used as input features and outputs for BBMs in (Lang et al., 2022).

Class	Description	Attributes
Input	Speed through water [knots]	V
	Mean draft [m]	T
	Trim [m]	$Trim$
	Heading [°]	HDG
	Significant wave height [m]	H_s
	Mean wave period [s]	T_z
	Mean wave direction [°]	D_{wave}
	Wind speed [m/s]	U_{wind}, V_{wind}
Output	Propulsion power [kW]	P_s

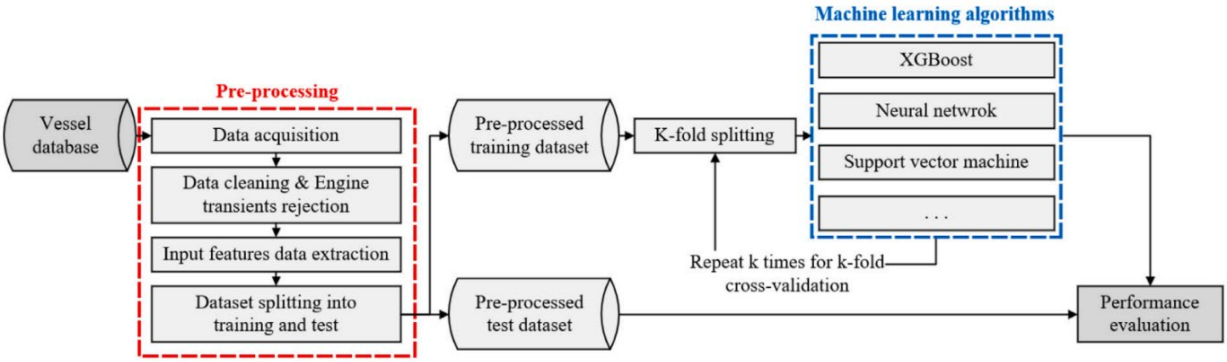

Figure 2.6: Workflow to derive BBMs for propulsion power prediction using ML algorithms (Lang et al., 2022).

Theoretical fuel model – fuel WBM

Following Eq. (2.6), the cost function can also be formulated to directly optimize overall fuel cost F_c. In this part, a theoretical speed-fuel ($V - F_c$) relationship is established. As in Eq. (2.6), to obtain F_c with a propulsion power P_s, the associated *SFOC* coefficient is required. A lower *SFOC* means higher fuel efficiency, i.e., the same power with less fuel, and conversely, a higher *SFOC* indicates lower fuel efficiency.

In this part, the cost function is further derived to calculate F_c. A theoretical cubic polynomial is first used to obtain *SFOC* from P_s, based on engine test data. The curve is shown in Figure 2.7, and denoted as:

$$SFOC = G_W(x),\ x = P_S \tag{2.12}$$

Thus, the fuel cost F_c can be obtained using Eq. (2.6):

$$F_C = P_S \times G_W(P_S) \tag{2.13}$$

$P_s = F_W(\boldsymbol{x})$ is modelled using the theoretical power WBM in Eq. (2.10), and put into the cubic curve $G_W(P_S)$ to find the associated *SFOC*. This fuel WBM is then obtained:

$$F_c = F_W(\boldsymbol{x}) \times G_W(P_S),\ P_S = F_W(\boldsymbol{x}),\ x = \{V\} \tag{2.14}$$

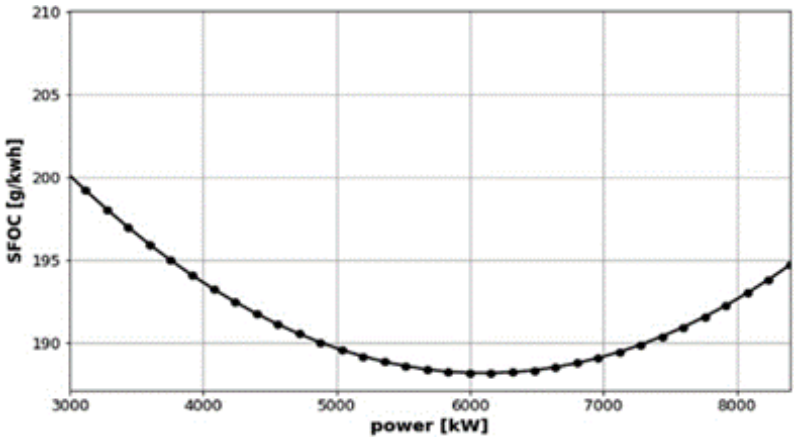

Figure 2.7: Theoretical polynomial *SFOC* curve used in this study.

ML power with theoretical SFOC model – fuel GBM

In the fuel GBM, the speed-power relationship is directly modelled using XGBoost method, i.e., the power BBM given in Eq. (2.11), and the associate *SFOC* coefficient remains the theoretical P_s– *SFOC* curve, i.e., Eq. (2.12).

As in Eq. (2.14), we replace the power WBM with the power BBM, and a fuel GBM is obtained:

$$F_c = F_{ML}(\boldsymbol{x}) \times G_W(P_S), \qquad P_S = F_{ML}(\boldsymbol{x}),$$
$$x = \{V, T, Trim, HDG, H_S, T_Z, D_{wave}, U_{wind}, V_{wind}\} \tag{2.15}$$

ML fuel model – fuel BBM

Many factors affect an engine's *SFOC*, including its type, design, and operating conditions, etc. For a marine diesel engine, *SFOC* is greatly influenced by actual operational parameters, and interactions with ship resistance and propulsion systems. Real-world conditions often differ from test conditions, leading to deviations in *SFOC* values because of factors such as load variations, sea state, hull condition (e.g., fouling, mechanical wear, and maintenance), and ambient temperature.

Accurate *SFOC* estimation is crucial for fuel consumption modeling. Inaccurate *SFOC* values can result in sub-optimal optimization with more fuel usage and deviations from scheduled ETAs. Dynamic marine environments necessitate continuous engine adjustments, further complicating *SFOC* predictions.

In this part, a data-driven *SFOC* model is developed based on the actual measurement data of SFOC, as presented in Figure 2.3:

$$SFOC = G_{ML}(x), \; x = P_S \tag{2.16}$$

Then, integrating with the XGBoost speed-power model in Eq. (2.11) following Eq. (2.6), a fuel BBM is presented as follows:

$$F_c = F_{ML}(\boldsymbol{x}) \times G_{ML}(P_S), \; x = \{V, T, Trim, HDG, H_S, T_Z, D_{wave}, U_{wind}, V_{wind}\} \tag{2.17}$$

This model can be used to compare with theoretical *SFOC* curves used in the fuel GBM given in Eq. (2.15), and investigate the impact of more accurate *SFOC* models on evaluating a ship's energy performance during actual voyages.

3 Methods for Isochrone-based voyage optimization

After constructing the ship energy cost model along with the cost function, we can integrate them into various optimization algorithms to achieve energy efficient objectives. In the following subsections, the original algorithm of Isochrone voyage optimization by Hagiwara (1989) is introduced, which is the focus and the foundation of this thesis. Five proposed improvement strategies follow, and the Isochrone-based predictive optimization algorithm is presented in the end.

3.1 The process of Isochrone algorithms

In the improved Isochrone method from Hagiwara (1989) (denoted as Isochrone method hereafter), the ship's speed is assumed to remain constant throughout the voyage, except for certain legs where adverse weather conditions may involuntarily affect the speed. The parameters that need to be defined before deployment are listed in Table 3.1, which will be introduced in the following algorithm process.

Table 3.1: Parameters to initialize the Isochrone algorithm.

Parameter	Description
Δt	Sailing time between two adjacent time stages
$\Delta\theta$	Change in heading angles between two consecutive sub-routes from each of the 'optimal' waypoints at the current time stage.
$2m+1$	Number of successor waypoints for each waypoint at the current stage
$2r$	Number of subsectors
ΔD	Width of the searching limit within each local subsector

Denote the departure location as $\boldsymbol{P_0}$ and the destination as $\boldsymbol{P_f}$, following Eq. (2.1). The great circle (GC) route between $\boldsymbol{P_0}$ and $\boldsymbol{P_f}$ is chosen as the reference route, denoted as GC_{ref}. For each (i^{th}) time stage, waypoints are given as $\boldsymbol{P}_{i,j}^{k}$, and it is derived from the latest ((i-1)$^{\text{th}}$) stage's point $\boldsymbol{P}_{i-1,\,k}$. Here, j in $\boldsymbol{P}_{i,j}^{k}$ means the j^{th} new point generated from the waypoint $\boldsymbol{P}_{i-1,\,k}$, where k refers to the k^{th} pre-reserved point at the (i-1)$^{\text{th}}$ isochrone $\{\boldsymbol{P}_{i-1}\}$.

The voyage is initially segmented into a sequence of time stages, i.e., T_i, where $i = 0, 1, \ldots, n, f$, from $\boldsymbol{P_0}$ to $\boldsymbol{P_f}$, as shown in Figure 3.1.T_0 represents the departure time and T_f represents the required time of arrival of the voyage.

Let a ship's initial service speed be denoted by V_s:

$$V_s = D/(T_f - T_0) \tag{3.1}$$

where D is the length of the reference great circle route GC_{ref}. The other inputs and outputs of the Isochrone algorithm are listed together in Table 3.2.

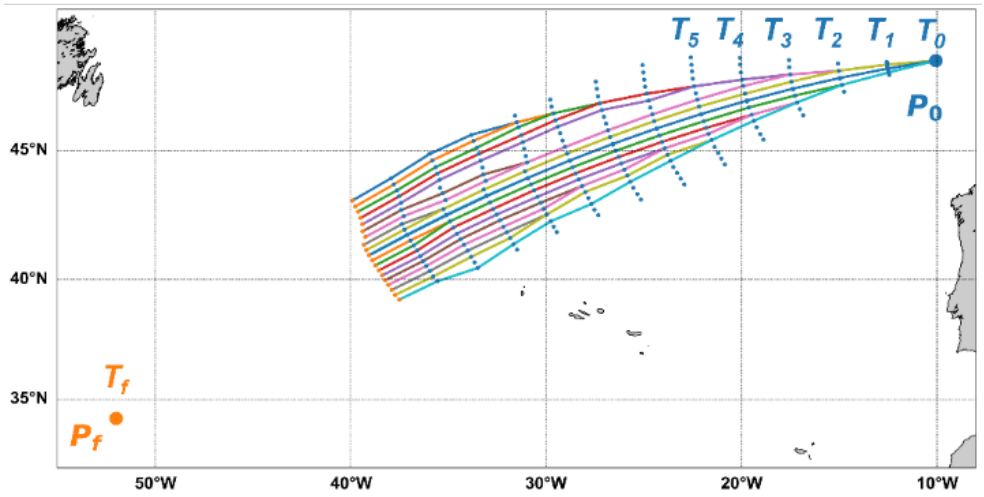

Figure 3.1: Voyage division in different time stages in the Isochrone method.

Table 3.2: Input features and output in the Isochrone algorithm.

Class	Description	Attributes
Input	Parameters to be initialized	In Table 3.1
	Departure waypoint	$\boldsymbol{P_0} = [x_0, y_0, T_0]$
	Destination waypoint	$\boldsymbol{P_f} = [x_f, y_f, T_f]$
	Service speed	V_s
Output	A series of waypoints consisting of the optimal voyage	$\boldsymbol{P_0}, \boldsymbol{P_1}, \boldsymbol{P_2}, \ldots, \boldsymbol{P_n}, \boldsymbol{P_f}$

Based on the above inputs and outputs, the process of the Isochrone voyage optimization is illustrated in Figure 3.2. The initial step is to generate the first isochrone $\{\boldsymbol{P_1}\}$ starting from $\boldsymbol{P_0}$ (Figure 3.2(a)):

At $\boldsymbol{P_0}$, head forward in the initial headings $\theta = \theta_{ref} \pm j \cdot \Delta\theta$ ($j = 0, 1, \ldots, m$) using the GC route to find new points for $\{\boldsymbol{P_1}\}$. θ_{ref} at this step is C_{ref} at $\boldsymbol{P_0}$, and C_{ref} is the initial course of GC_{ref} at $\boldsymbol{P_0}$.

1) Verify the sailing constraints:
   a) Check if V_s can be achieved with the headings θ under the weather at $\boldsymbol{P_0}$. If not, adjust the speed V_s in accordance with engine limitations.
   b) Check for land-crossing, shallow water, no-go zones, etc.
2) Proceed from $\boldsymbol{P_0}$ for Δt hours, with headings θ and speed V using the GC route. Waypoints of the first isochrone $\{\boldsymbol{P_1}\}$, i.e., $\{\boldsymbol{P_{1,k}}, k = 1, 2, \ldots, 2m+1\}$ are found. Link $\boldsymbol{P_0}$ to every $\boldsymbol{P_{1,k}}$ with directions from $\boldsymbol{P_0}$ to $\{\boldsymbol{P_1}\}$ using an edge/sub-route.

The next step is navigating from each waypoint in $\{\boldsymbol{P_1}\}$ following the same steps as above; potential waypoints $\{\boldsymbol{P_{2,j}^k}, k = 1, 2, \ldots, 2m+1, j = 1, 2, \ldots, 2m+1\}$ can also be obtained to opt for $\{\boldsymbol{P_2}\}$. To

prevent the exponential growth of waypoints and perform the selection, the sub-sector is introduced (Hagiwara, 1989), which comprises sub-areas distributed evenly around GC_{ref}. Thus, starting from $\{\boldsymbol{P_1}\}$, the voyage search is carried out as follows.

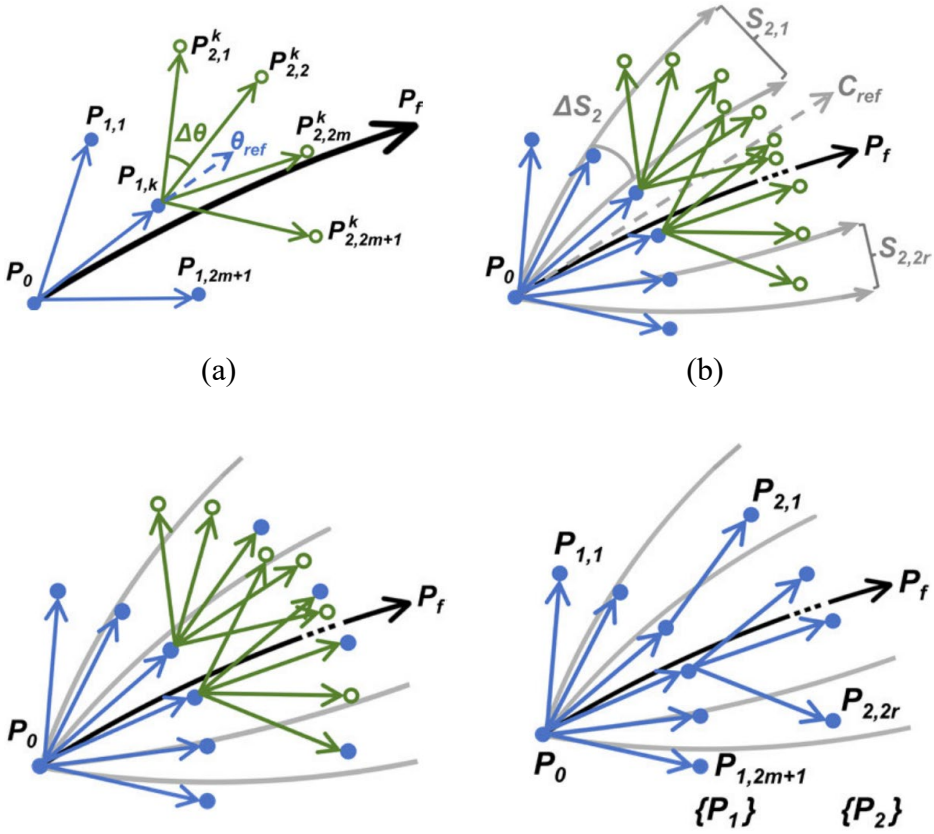

Figure 3.2: Generation of waypoints in the Isochrone algorithm.

1) Repeat the processes above as in Figure 3.2(a) at each (k^{th}) waypoint $\boldsymbol{P_{1,k}}$. The reference heading θ_{ref} is the arrival course at $\boldsymbol{P_{1,k}}$ from $\boldsymbol{P_0}$. Each $\boldsymbol{P_{1,k}}$ leads to $2m+1$ potential waypoints $\{\boldsymbol{P_{2,j}^k}$, $j = 1, 2, \ldots, 2m+1\}$.
   Sub-sectors are defined based on $2r+1$ initial courses $C_{ref} \pm k{\cdot}\Delta S_i$ ($k= 0, 1, \ldots, r$) of the GC route from $\boldsymbol{P_0}$, shown as grey lines in Figure 3.2(b).
2) The increment ΔS_i ($i = 2$, indicating the second time stage) is defined following (Hagiwara, 1989):

$$\Delta S_i = c * \Delta D \;/\; sin\,(c * d_i),\; c = \pi \;/\; (60 * 180) \tag{3.2}$$

   where d_i ($i = 2$) is the expected traveled distance equal to $i*\Delta t*V_s$ ($i = 2$).
   Then, subsectors $\{\boldsymbol{S_{i,k}}\}$ are given based on sub-areas between GC routes with adjacent initial headings, i.e., $[C_{ref} + (k\text{-}r\text{-}1){\cdot}\Delta S_i,\ C_{ref} + (k\text{-}r){\cdot}\Delta S_i]$, ($i =2$, $k =1, 2, \ldots, 2r$).
3) In each (k^{th}) sub-sector $S_{2,k}$, identify the optimal waypoint $\boldsymbol{P_{2,k}}$ with the optimum cost given by the cost function C in Eq. (2.5), shown as blue dots in Figure 3.2(c).

4) Only optimal waypoints $\{P_{2,k}, k = 1, 2, \ldots, 2r\}$ are pre-reserved. Connect by directed edges with its predecessor in $\{P_1\}$ respectively, as shown in Figure 3.2(d). The second isochrone $\{P_2\}$ is obtained.

Repeatably, based on the isochrone $\{P_2\}$, and follow the above steps in recursion: at the i^{th} time stage, generate waypoints $\{P_{i,j}^k, k = 1, 2, \ldots, 2r, j = 1, 2, \ldots, 2m+1\}$, and identify the isochrone $\{P_{i,k}, k = 1, 2, \ldots, 2r\}$ from $\{P_{i,j}^k\}$ using sub-sectors $\{S_{i,k}\}$. New isochrones are generated in sequence, until the destination is reached.

3.2 Strategies to improve Isochrone algorithms

The Isochrone optimization method addresses the issue of unlimited waypoints, as discussed in Chapter 1.2.2. Specifically, the number of candidate points at each time stage originally increases exponentially. The Isochrone optimization method mitigates this issue by using subsectors to selectively choose waypoints. However, some shortcomings are still evident, e.g., sub-routes continuously widen as they extend, covering a vast search area. When approaching the endpoint, waypoints connect directly to the destination. This often results in routes with sharp turns near the destination, as shown in Figure 3.3.

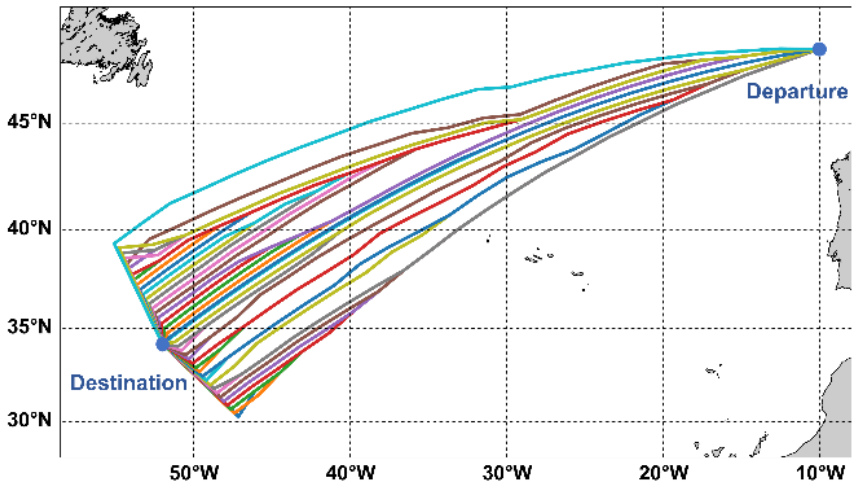

Figure 3.3: Routes generated using the Isochrone method featuring sharp turns near the destination.

Clearly, most of those candidate routes with abrupt direction changes are not realistic as practical voyage. To solve the problem, five strategies to improve the Isochrone method are investigated in the following subchapters respectively, as summarized in Figure 3.4 and Table 3.3, to accomplish the following objectives:

1) Remain computationally efficient,
2) Avoid the route convergence problem in Figure 3.4,
3) Improve the optimization performance and avoid local optimizations.

Table 3.3: Comparison of the optimization process for each improvement strategy.

Modification	First Half Voyage	Second Half Voyage		Final Stage
		Subsector	Searching method	
Reversed subsectors	Isochrone method	Reversed subsectors	Isochrone method	$\Delta\theta = \Delta\theta \cdot 10\%$
Optimal subsectors			Reserve suboptimal nodes	
Isochrone-A*			Augmented heuristic function	
Power subsectors		-	Optimal power greedy search	
Isochrone-Dijkstra		Dijkstra algorithm		

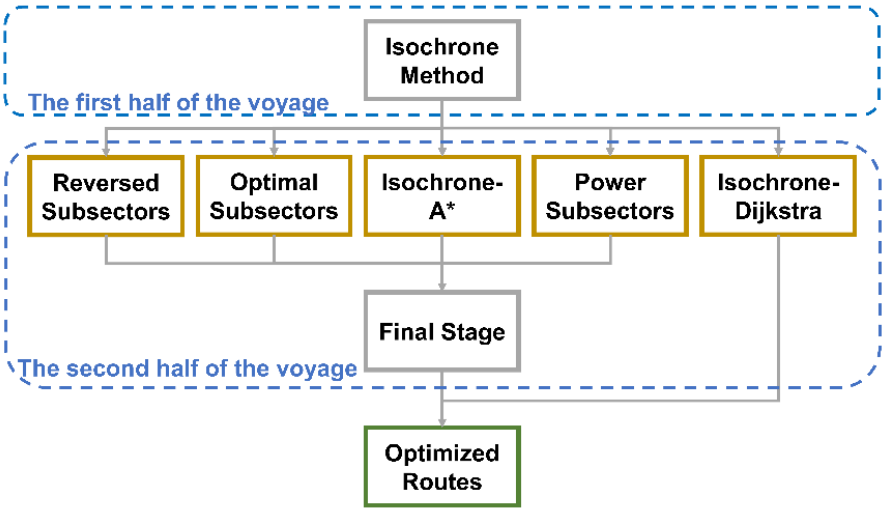

Figure 3.4: Improvement strategies of the Isochrone method.

3.2.1 Reversed subsectors

The sharp turns appear because, in the Isochrone method, the subsector is defined as a monotonically increasing function of sailing distance d_n, thus it keeps expanding without decreasing. In this part, the subsectors in the late stages of a voyage are reformulated to resolve this problem.

In the second half of the voyage, the distance from the departure $\boldsymbol{P_0}$ is calculated, i.e., d_i is replaced by the current distance to $\boldsymbol{P_f}$ (denoted as d_{iS}), which is then used to define the width of the following subsectors in the second half of a voyage:

$$d_{iS} = d_{total} - d_i, \Delta S_{iS} = \frac{c \cdot \Delta D}{\sin(c \cdot d_{iS})} \tag{3.3}$$

where d_{total} is the total distance from $\boldsymbol{P_0}$ to $\boldsymbol{P_f}$. along the reference route. A symmetric subsector set is generated as shown in Figure 3.5, which reduces its range when approaching the endpoint.

The procedure for this improved method is given as follows, with a flowchart in Figure 3.6:

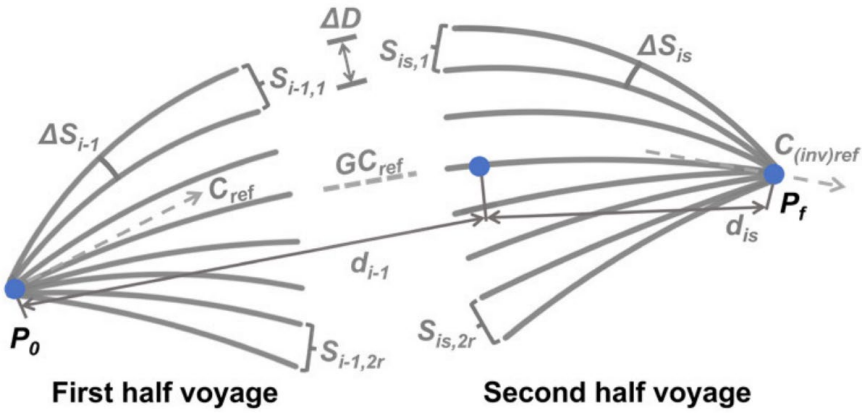

Figure 3.5: Reversed subsectors generated during the second half voyage.

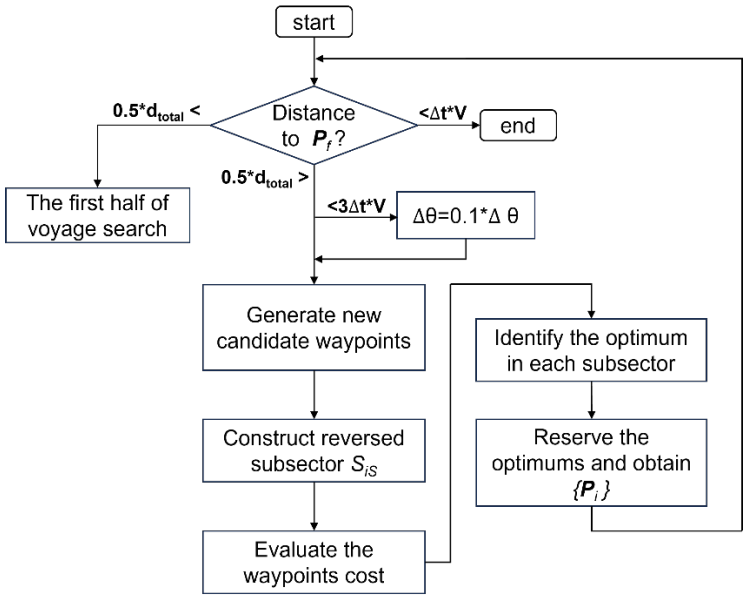

Figure 3.6: Flowchart of Reversed subsector method.

1) Conduct the steps in subchapter 3.1 for the voyage's first half. If the distance between the current isochrone and P_f falls below 0.5* d_{total}, use the reversed subsectors are used.
2) From each waypoint at the current i^{th} time stage, i.e., $P_{i,k}$, generate new waypoints for the $(i+1)^{th}$ time stage following headings $C_{ni} \pm j \cdot \Delta\theta$ ($j=0, 1, \ldots, m$). Each $P_{i,k}$ derives $2m+1$ new points $\{P^k_{i+1,j}, j = 1, 2, \ldots, 2m+1\}$.
   C_{ni} denotes the initial course at the current waypoint $P_{i,k}$, along the GC route to P_f.
3) Denote the reversed subsectors based on the back azimuth angles as $C_{inv} \pm k \cdot \Delta S_{(i+1)\,S}$ ($k= 0, 1, \ldots, r$), where C_{inv} is the azimuth angle of the back course at P_f, i.e., from P_f to P_0 along GC_{ref}, and calculate $\Delta S_{(i+1)\,S}$ using Eq. (3.3).
   $2r$ reversed subsectors $\{S_{(i+1)\,S}\}$ are outlined by each pair of the adjacent back course heading angles, i.e., $C_{inv}+(k-r-1) \cdot \Delta S_{(i+1)\,S}$ and $C_{inv}+(k-r) \cdot \Delta S_{(i+1)\,S}$ ($k =1, 2, \ldots, 2r$).

4) In each subsector of $\{S_{(i+1)S}\}$, choose the minimum cost waypoint to form the isochrone $\{\boldsymbol{P}_{i+1}\}$ at the $(i+1)^{th}$ time stage. The waypoint selection criterion is the shortest distance to the destination, to avoid any detour leading to high fuel consumption.
5) Repeat the above steps 1) - 4). If the current distance to $\boldsymbol{P_f}$ is less than $3{\cdot}\Delta t{\cdot}Vs$, reduce $\Delta\,\theta$ to 10% of its current value as the reverse subsectors are compact around $\boldsymbol{P_f}$.
6) When the current distance to $\boldsymbol{P_f}$ is less than $\Delta t{\cdot}Vs$, connect waypoints to $\boldsymbol{P_f}$.

3.2.2 Optimal subsectors

Constructing reversed subsectors, however, is found to cause the subsectors to become very narrow at late stages. Consequently, only a few isochrone waypoints that are locally optimal would be chosen in these compact subsectors. Therefore, generated sub-routes generated may all originate from these locally optimal waypoints. However, an ideal optimization algorithm should suggest candidate routes that cover sufficient sailing areas.

The following method to define, optimal subsections, is proposed for the above problem, with a flowchart in Figure 3.7:

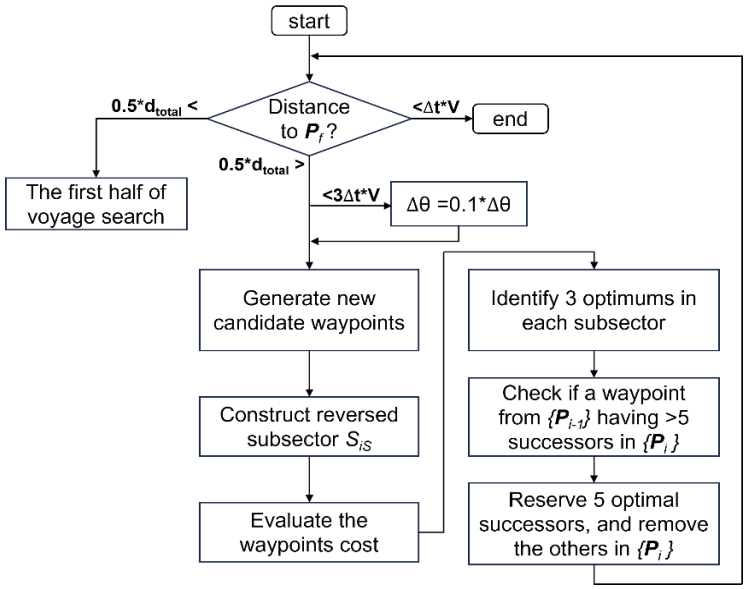

Figure 3.7: Flowchart of Optimal subsector method.

1) Generate the waypoint grid as in subchapter 3.1. The optimal waypoint is the closest to the destination.
2) In the latter half of the voyage, define the number of nodes/waypoints in each subsector, instead of only one in the first half. This value is set to three in the following case study.
3) Restrict the number of successors that can be reserved for one predecessor, to prevent dominance. This value is set to five in the case study.

3.2.3 Isochrone-A* method

In addition to modifying the subsectors, another approach is to explore different criteria for selecting optimal waypoints in subsectors, i.e., changing cost functions. Currently, the selection criterium for the Isochrone voyage optimization methods is defined as either the shortest distance to the destination or the minimum fuel consumed at the current waypoints. That is, it considers only the past information of the voyage. This study investigates the inclusion of a heuristic term to account for future considerations as well.

This strategy relies on the concept of the A* algorithm, a widely used graph-searching and an informed search algorithm. It introduces a cost function that includes both forward and backward cost estimation along the search routes:

$$f(n) = g(n) + h(n), \tag{3.4}$$

where $g(n)$ is the consumed cost from the departure, and $h(n)$ is the heuristic term estimating the cost to reach the destination. The procedures are presented in the flowchart in Figure 3.8. The waypoint is generated by the same approach as subchapter 3.1, and the changes are made in the cost function:

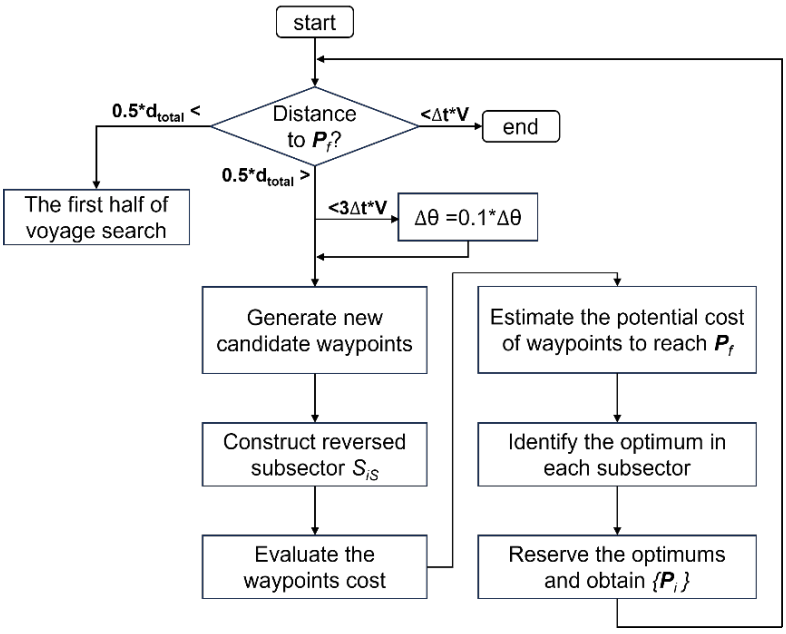

Figure 3.8: Flowchart of Isochrone-A* method.

(1) In the first half of the voyage, conduct the same procedures as Reverse subsectors approach.
(2) In the second half voyage, the cost $f(n)$ is added with a heuristic term $h(n)$:
- $g(n)$: the accumulative fuel consumption from departure.
- $h(n)$: the estimation of the fuel consumption to $\boldsymbol{P_f}$, assuming a GC route from the current position to $\boldsymbol{P_f}$ and taking into account weather changes at each time stage.
- $f(n)$: the estimated overall fuel consumption.

3.2.4 Power subsectors

To avoid issues of local optimization for one predecessor in the latter half of the voyage, an alternative method is proposed, referred to as "power subsectors." This method selects the optimal point within the successors for each waypoint, ensuring that each preceding waypoint forms a feasible route to reach $\boldsymbol{P_f}$. The approach can be implemented as follows, as illustrated in Figure 3.9.

1) In the first half of the voyage, conduct the same procedures as Reverse subsectors approach.
2) In the latter half, every waypoint proceeds towards $\boldsymbol{P_f}$ following the heading $C_{ni} \pm j \cdot \Delta\theta$ ($j=0, 1, \ldots, m$). Then, among $2m+1$ successors, keep the point with the lowest fuel cost, and append it as the optimal one. Continue towards $\boldsymbol{P_f}$.

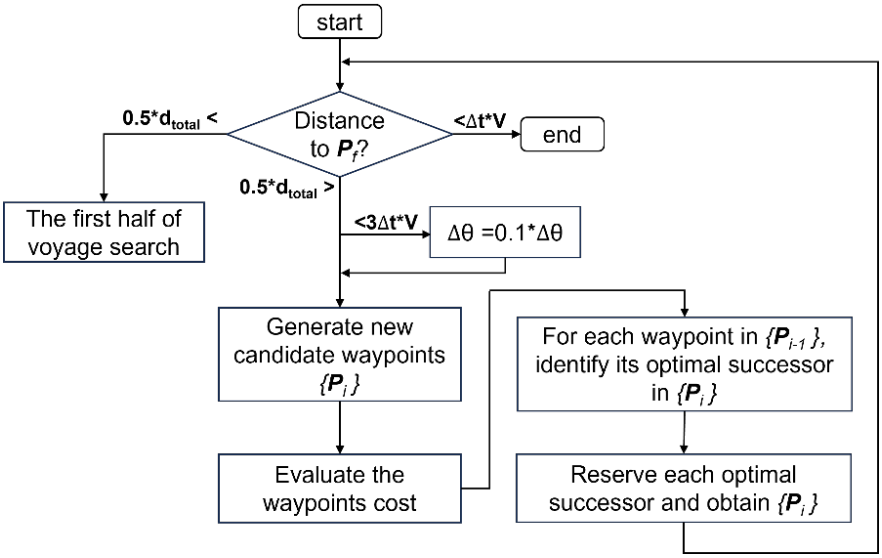

Figure 3.9: Flowchart of Power subsectors method.

3.2.5 Isochrone-Dijkstra method

In the Isochrone algorithm, waypoints are generated in a tree structure. Removing a waypoint leads to the removal of all its predecessors, thereby limiting the search for future alternatives. To address this issue, this approach implements Dijkstra's algorithm for the second half of the voyage to ensure a reasonable search range, as shown in Figure 3.10.

The Dijkstra method starts by initializing a static grid based on the sailing area, where edges are weighted according to the fuel cost of the corresponding sub-routes. Within this static grid, the Dijkstra algorithm can determine the lowest cost route between two waypoints by evaluating every possible route. This approach is executed following the flowchart in Figure 3.11:

1) In the first half of the voyage, apply the same procedures apply.

2) In the second half, generate a static grid as in Figure 3.10. Obtain the waypoints in subsequent stages by translating the latest isochrone in the direction of the GC_{ref} towards $\boldsymbol{P_f}$.
3) Assign a cost for all sub-routes based on the estimated fuel cost. Apply the Dijkstra algorithm to find the lowest cost route, starting from each waypoint in the latest isochrone to $\boldsymbol{P_f}$ respectively.
4) This will yield several potential sailing routes. These candidate half-routes possess different ETAs as the distance varies in sub-routes, and sailing speed is constant. Choose the optimal route as the route with the closest ETA to the required arrival time.

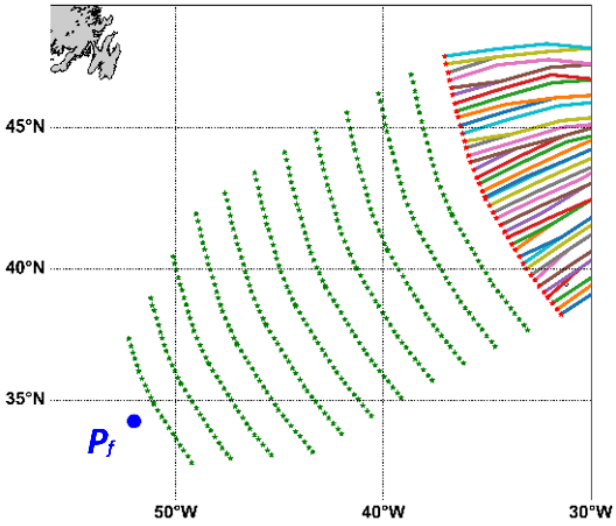

Figure 3.10: Static grid initialized at the latter half voyage for the Dijkstra algorithm.

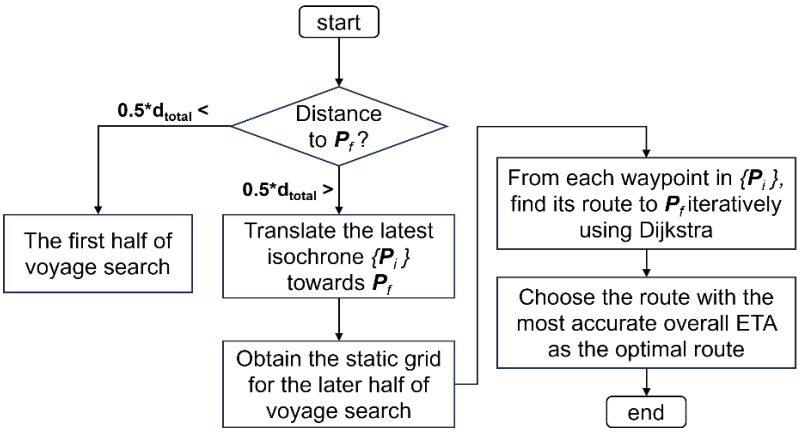

Figure 3.11: Flowchart of Isochrone-Dijkstra method.

3.3 Isochrone-based predictive optimization

This method is developed based on the above conducted research. Firstly, based on the investigation of ship models in Chapter 2, the model chosen in this method is a state-of-the-art GBM, which predicts the fuel consumption to evaluate the energy efficiency for ship sailings. This GBM will be

further introduced in detail in Chapter 4.3.1, the findings of comparing ship models will be presented in Chapter 4.1 and Chapter 5. Secondly, based on the comparisons of improving strategies, introduced in Chapter 3.2, the waypoint grid partition strategies in Chapter 3.2.1 and the refined cost function in Chapter 3.2.3 are combined, to prevent sharp route turnings and local optimizations. Finally, a predictive optimization approach is developed, leading to the Isochrone-based voyage predictive optimization (IPO) algorithm, which improves performance in real-time multi-objective voyage optimization.

Isochrones of the first half voyage in the IPO method

The first phase of the IPO method proceeds as shown in Figure 3.2. The cost function C is defined to identify the waypoint nearest to $\boldsymbol{P_f}$. The objective is to minimize the deviation from $\boldsymbol{P_f}$ at the initial stages of the voyage, as deviations can result in a much longer and more fuel-consuming route.

Isochrones of the second half voyage in the IPO method

When $d_{iS} < 0.5D$, the second half of the voyage search begins. At this stage, special attention needs to be given to two problems: 1) ensuring the convergence of the route towards $\boldsymbol{P_f}$, and 2) avoiding local optimization. The reversed subsector is adopted for problem 1) following Figure 3.1, and predictive optimization is integrated to address problem 2), as shown in Figure 3.12.

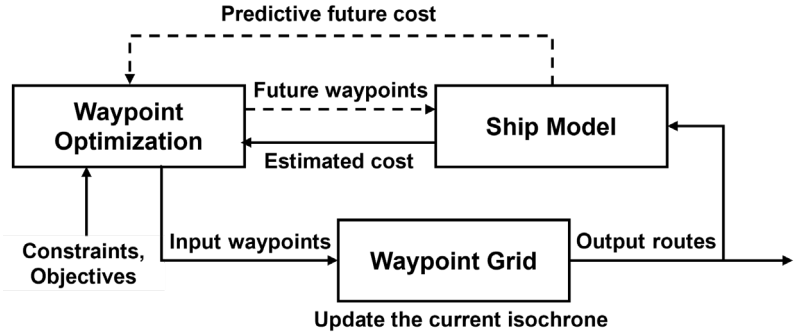

Figure 3.12: Flowchart of predictive optimization used in the IPO method.

Similar to the Isochrone A* method in subchapter 3.2, the cost not only considers the local/partial cost of reaching a waypoint, but also predicts the future cost to reach $\boldsymbol{P_f}$, which is incurred after choosing the waypoint. The cost function C_p is augmented with a heuristic term $h\,(\boldsymbol{S})$:

$$C_p = \int_{T_0}^{T_i} j(\boldsymbol{S})dt + h(\boldsymbol{S}) \tag{3.5}$$

where $\int_{T_0}^{T_n} j(\boldsymbol{S})dt$ accumulates the consumed fuel from $\boldsymbol{P_0}$ to $\boldsymbol{P_{i,k}}$, h $(\boldsymbol{S})$ predicts the future fuel needed to reach $\boldsymbol{P_f}$ from $\boldsymbol{P_{i,k}}$. This prediction relies on the ship model and weather forecasts, assuming the vessel adheres to the GC route and incorporates dynamic weather updates at each time stage. Consequently, the cost C_p estimates the total fuel consumption from $\boldsymbol{P_0}$ to $\boldsymbol{P_f}$. To avoid local optimization, as depicted in Figure 3.13, the predictive cost of each waypoint is considered, taking into account the dynamic effects of weather and distance.

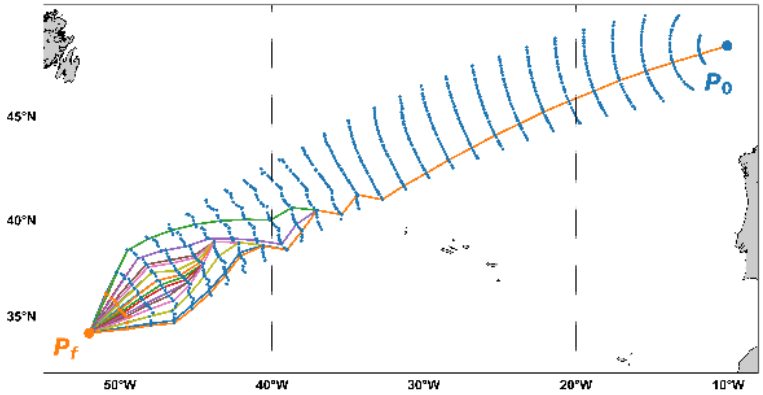

Figure 3.13: Example of a local optimized result giving overlapped candidate routes.

The second half of the voyage search is outlined as follows, given the current(i^{th}) isochrone:

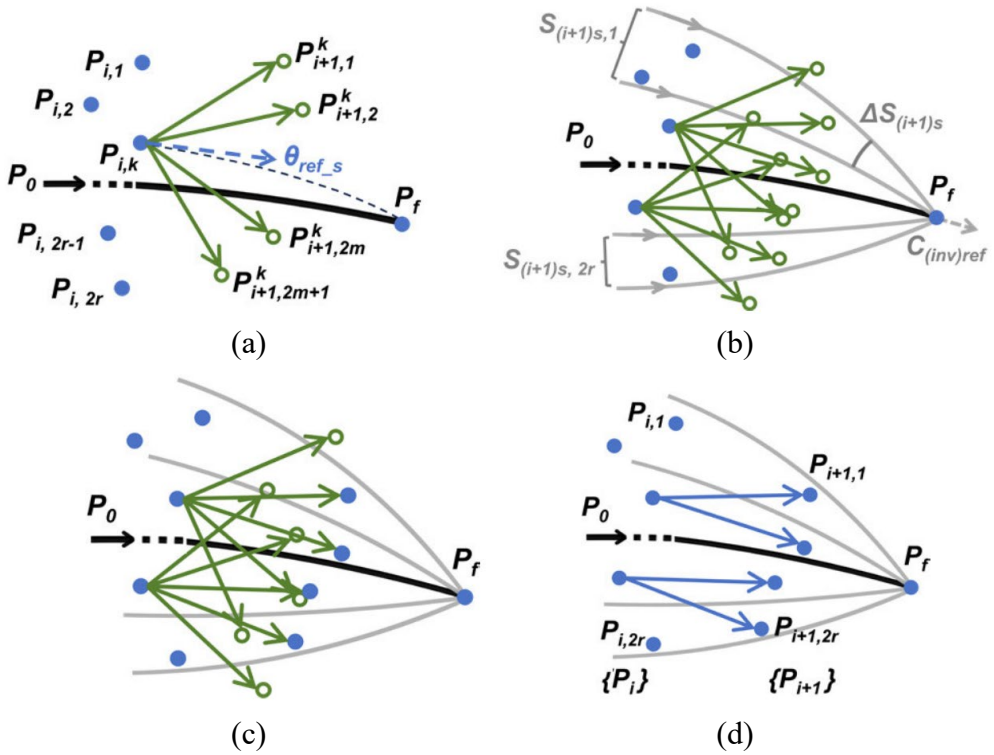

Figure 3.14: Generation of isochrones in the second half of the voyage using the IPO method.

1) At current waypoint $\boldsymbol{P_{i,k}}$ (k^{th} waypoint in the i^{th} isochrone), follow the heading $\theta=\theta_{ref\_s} \pm j\cdot\Delta\theta$ ($j= 0, 1, \ldots, m$) and obtain the new waypoints for the next/($i+1$) th stage.

θ_{ref_s} is the initial course of the GC route from $\boldsymbol{P_{i,k}}$ to $\boldsymbol{P_f}$. Each $\boldsymbol{P_{i,k}}$ generates $2m+1$ new points $\{\boldsymbol{P}^{k}_{i+1,j}, j = 1, 2, \ldots, 2m+1\}$ as in Figure 3.14(a).

2) The reversed sub-sectors are indicated by $2r+1$ GC routes with arrival courses $C_{inv(ref)} \pm k{\cdot}\Delta S_{(i+1)\,s}$ ($k= 0, 1, \ldots, r$) at $\boldsymbol{P_f}$, as shown by the grey lines in Figure 3.14(b).
Calculate $\Delta S_{(i+1)\,s}$ with Eq. (3.3), and define the sub-sectors $\{\boldsymbol{S}_{(i+1)\,s,\,k}\}$ as sub-areas between adjacent arrival headings at $\boldsymbol{P_f}$, i.e., $[C_{inv(ref)} + (k\text{-}r\text{-}1)\cdot\Delta S_{(i+1)\,s}, C_{inv(ref)} + (k\text{-}r)\cdot\Delta S_{(i+1)\,s}]$, ($k = 1, 2, \ldots, 2r$).

3) In each sub-sector $S_{(i+1)\,s,\,k}$ (k^{th} sub-sector at $(i+1)^{\text{th}}$ time stage), choose the optimal point $\boldsymbol{P_{i+1,\,k}}$ as the least cost one, using the cost function C_p defined in Eq. (3.5), as shown by the blue dots in Figure 3.14(c).

4) Connect each optimal points $\{\boldsymbol{P_{i+1,k}}, k = 1, 2, \ldots, 2r\}$ with its predecessor, as shown in Figure 3.14 (d), obtaining the next/$(i+1)^{\text{th}}$ isochrone $\{\boldsymbol{P_{i+1}}\}$.

A feasible route set $\{\boldsymbol{R}\}$ is generated, with all candidate routes having comparable ETA. For each sub-route, fuel consumption is calculated based on the local weather conditions at the starting way-point. The total fuel consumption is the sum of all sub-routes' cost, i.e., a sequence from $\boldsymbol{P_0}$ to $\{\boldsymbol{P_1}\}$, $\{\boldsymbol{P_1}\}$ to $\{\boldsymbol{P_2}\}$, …, $\{\boldsymbol{P_n}\}$ to $\boldsymbol{P_f}$, as shown in Figure 3.15. The optimal solution $\boldsymbol{R^*}$ has the lowest accumulative fuel.

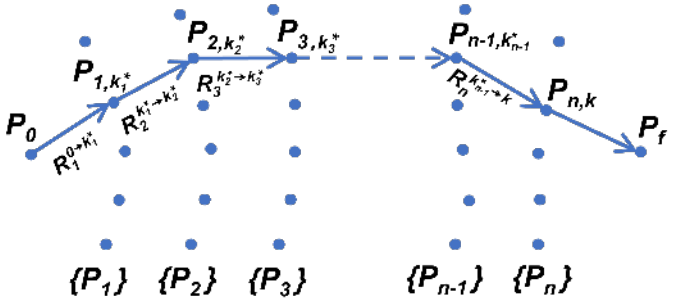

Figure 3.15: Examples of the optimal route R^*.

4 Results from appended papers

Based on the presented methods in ship modelling and voyage optimization algorithm, this chapter summarizes the major findings and results of the methods, from appended Papers I-III respectively in the following subsections.

The overall workflow for appended research papers I-III is illustrated in Figure 4.1. Using methods introduced in Chapter 2.3, Paper I investigates the sensitivity and impact of various ship energy cost models on the voyage optimization algorithm. Paper II proposes and compares five strategies to improve the Isochrone method. Based on these findings, Paper III presents a predictive optimization method based on the Isochrone approach for enhancing energy efficiency in ship voyage planning and execution. The works included in this thesis are described in the red box in Figure 4.1. Future studies are presented in the green box, with details in Chapter 6.

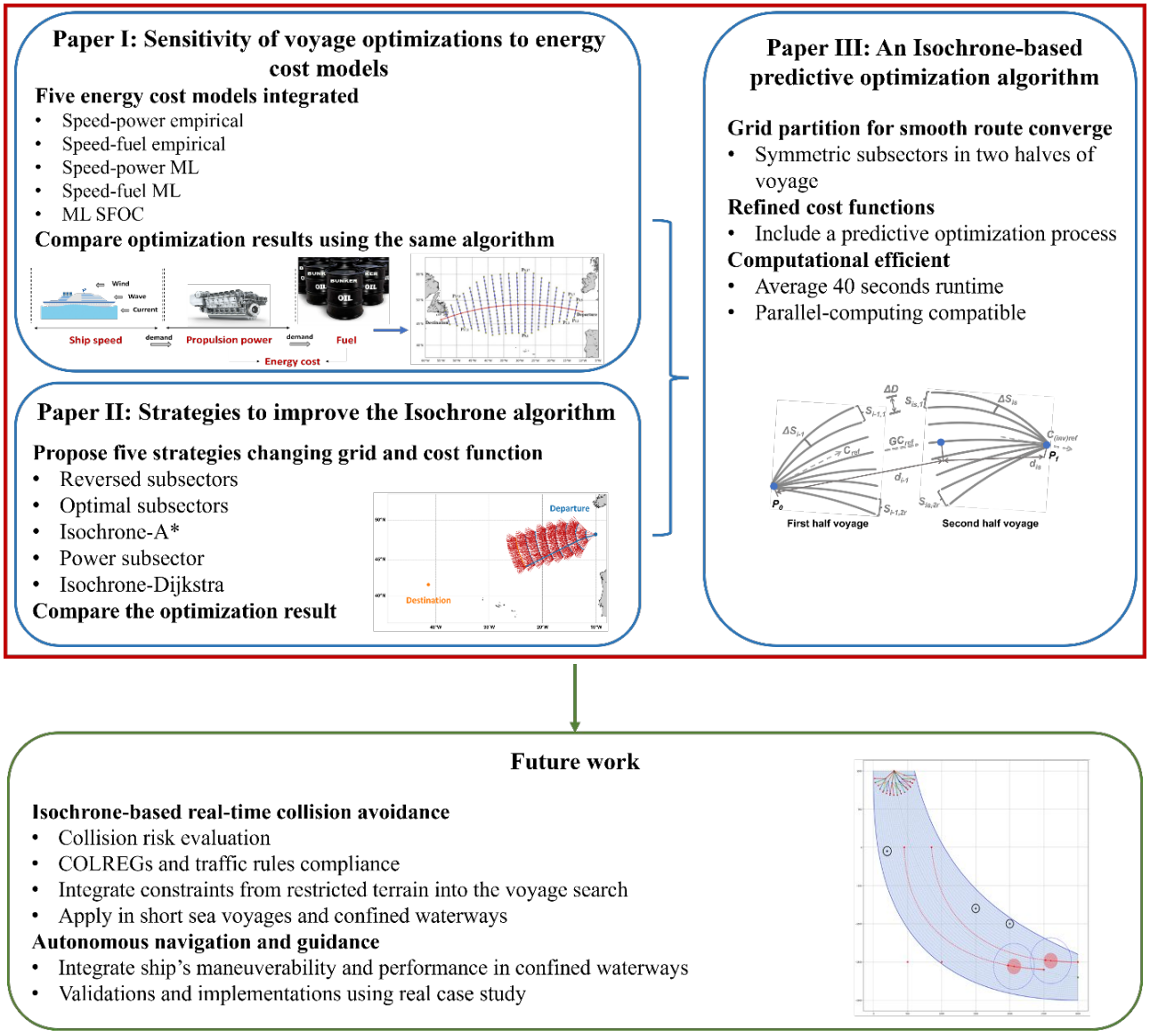

Figure 4.1: The outline of the research presented in this thesis.

Case studies are conducted for result validation in each of the appended papers, focusing on a chemical tanker with full-scale measurements, operating in the North Atlantic. The ship specifications are detailed in Table 4.1. The ship's operation is guided by a conventional voyage optimization system and the ship crews onboard. Its actual routes have been planned and chosen based on the crew's experience, and the actual ship has certain voyage optimization capabilities.

The study includes six voyages of the ship in 2015 and 2016 as shown in Figure 4.2. These voyages cover eastbound and westbound trips across winter and summer, encompassing a range of environmental conditions such as calm, moderate, and severe sea states. Additionally, weather data, including wind, wave, and current, are necessary to describe sailing environments and estimate ship performance. Historical meteorological and oceanographic data from 2015 and 2016 were retrieved in 2023 from the ECMWF ERA-5 dataset for wind (speed and direction) and wave (height, direction, and period), and from Copernicus 2023 server (http://marine.copernicus.eu/) for current.

Table 4.1: Principal particulars of the chemical tanker ship.

Length	178.4 m	Design draught	10.98 m
Length	174.8 m	Block coefficient	0.8005
Beam	32.2 m	Deadweight	50752 t
Depth	17.0 m		

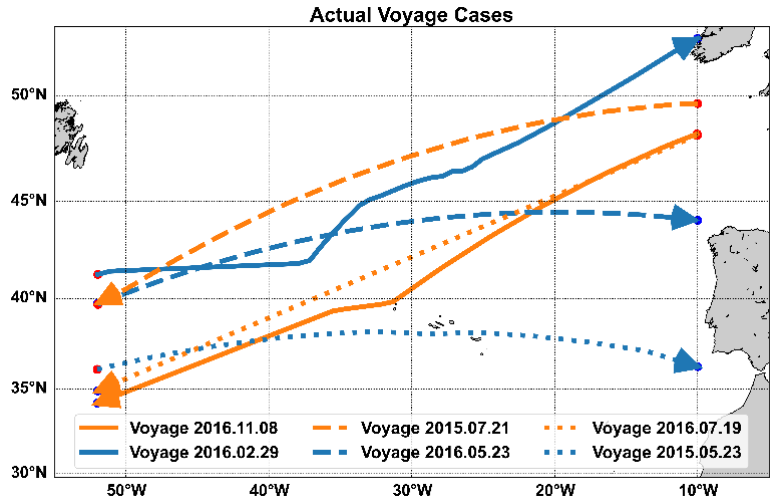

Figure 4.2: Actual case study voyages used in the thesis for validations.

4.1 Summary of Paper I

Paper I investigates the sensitivity of ship voyage optimizations to different energy cost functions derived from various modeling techniques. The chemical tanker with full-scale measurement data, as presented in Table 4.1, is used in the case study to examine the sensitivity of voyage optimizations regarding energy efficiency. The study employes different energy cost functions, i.e., total power or fuel consumption, built by different modeling techniques. The paper provides detailed insights into

using different energy cost functions and models, offering practical recommendations for the model used in voyage optimization.

Results for westbound voyages

Two westbound voyages, Voyage 2015.07.21and 2016.11.08 are studied. The optimized routes using different models are presented in Figure 4.3, with encountered weather (represented by significant wave height H_s) compared in Figure 4.4. The optimization results are summarized in Table 4.2, where the fuel consumption is given both in amount and the percentage of savings compared to the actual fuel cost.

Table 4.2: Comparison of using different energy cost models.

Category	Models	Fuel consumption [ton]			
		Voy. 2016.11.08		Voy. 2015.07.21	
		Amount	%	Amount	%
	Actual ship	177.9	-	178.5	-
Power as cost	Power WBM	163.1	8.4	178.0	0.3
	Power BBM	154.6	13.1	151.4	15.2
Fuel as cost	Fuel WBM	162.3	8.8	165.9	7.0
	Fuel GBM	154.3	13.3	151.3	15.2
	Fuel BBM	161.3	9.3	161.3	9.6

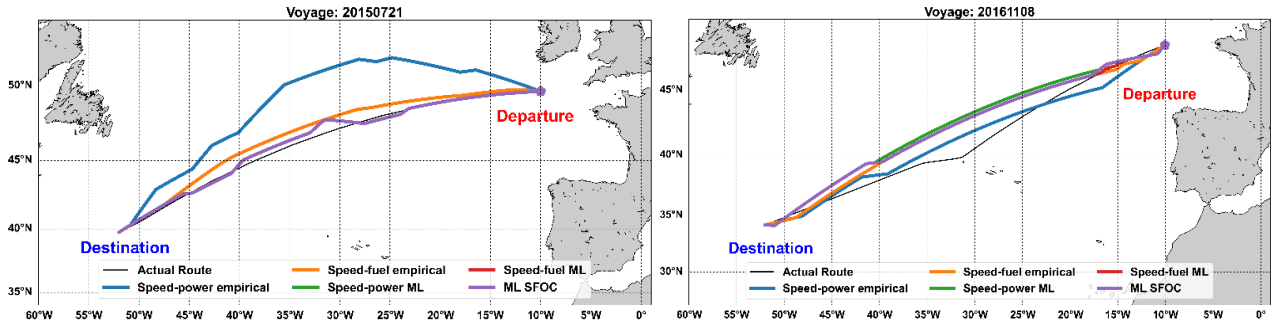

Figure 4.3: Optimized routes using different energy cost models for Voyage 2015.07.21 (left) and 2016.11.08 (right).

The study evaluates fuel savings using five cost functions, two derived from empirical knowledge and three derived from ML techniques: ML speed-power, speed-fuel models, and ML *SFOC* model. In both two westbound voyage cases, these ML-based models show higher fuel reduction. Specifically, for the summer Voyage 2015.07.21 with more variable sea conditions, fuel consumption differences are more pronounced compared to the calmer Voyage 2016.11.08: the empirical speed-power model offers 0.3% fuel savings, whereas the speed-fuel model shows 7.0% savings. ML models yield approximately 13% and 15% fuel savings in both cases, though considering *SFOC* effects

adjusts these to around 9%. Routes derived from empirical models for optimizing power and fuel diverge significantly, often not overlapping. Notably, the speed-power empirical route in Figure 4.3 takes a long detour, resulting in minimal savings (0.3%) due to local optimization prioritizing lower power over distance, and this route consequently encounters lower waves. Conversely, ML model routes are more consistent, closely overlapping and showing similar fuel savings and sea states. However, differences in fuel consumption estimates arise from including actual *SFOC* values, leading to varied savings.

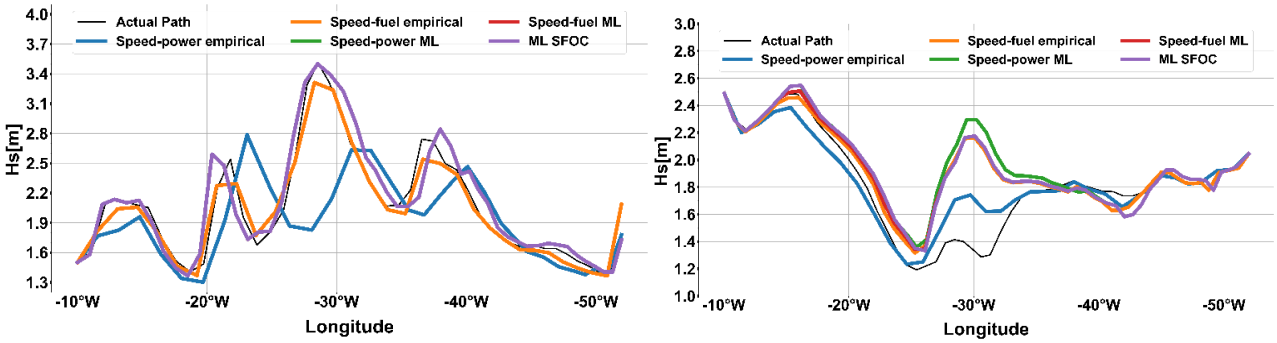

Figure 4.4: Encountered H_s using different energy cost models along Voyage 2015.07.21 (left) and 2016.11.08 (right).

Results for eastbound voyages

Two east voyages, Voyage 2016.02.29 and 2016.05.23 are shown in this section. The optimized routes using different models are presented in Figure 4.5, with encountered weather (significant wave height H_s) compared in Figure 4.6. The optimization results are summarized in Table 4.3.

Table 4.3: Comparison of using different energy cost models.

Category	Models	Fuel consumption [ton]			
		Voy. 2016.02.29		Voy. 2016.05.23	
		Amount	%	Amount	%
	Actual Ship	174.8	-	174.2	-
Power as cost	Power WBM	152.0	13.0	152.0	12.7
	Power BBM	145.3	16.9	149.4	14.2
Fuel as cost	Fuel WBM	151.8	13.2	150.9	13.4
	Fuel GBM	143.7	17.8	149.2	14.4
	Fuel BBM	150.6	13.8	158.8	8.8

In these two eastbound voyages, the fuel savings from the two empirical models (speed-power and speed-fuel) are both around 13%. Despite this similarity, differences in routes and encountered weather conditions are evident. The empirical models are less effective in improving energy

efficiency compared to ML cost functions, similar to the westbound cases. Using ML speed-power and speed-fuel models results in approximately 17% and 14% fuel reductions, respectively, for the two cases. These models consistently show close fuel savings but suggest different routes and encounter different environmental conditions, especially in Voyage 2016.02.29. Including *SFOC* calculations with ML techniques in this voyage increases fuel reduction to 13.8% and suggests a completely different route, as shown in Figure 4.5. This is likely due to the significant environmental changes of Voyage 2016.02.29 affecting *SFOC* values, leading to varied optimization results. Conversely, in Voyage 2016.05.23, the ML *SFOC* model results do not show significant deviations, with sea conditions overlapping those of the ML speed-fuel model. Both eastbound voyages involve greater environmental changes than the westbound cases, highlighting more apparent deviations between optimizing for power versus fuel cost.

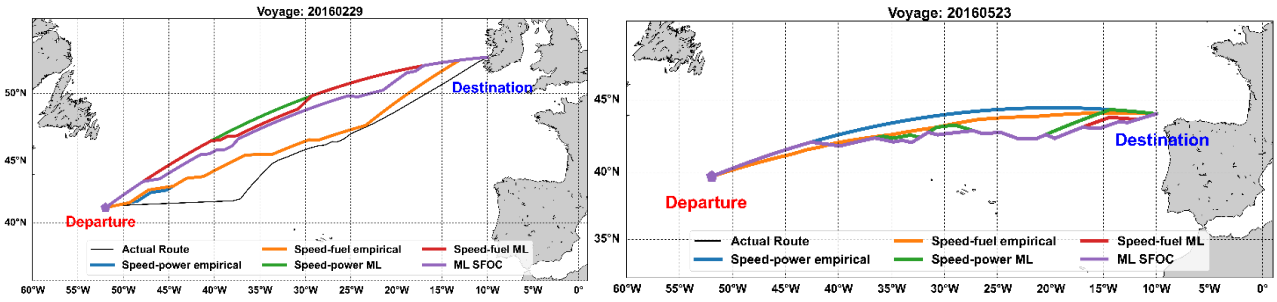

Figure 4.5: Optimized routes using different energy cost models for Voyage 2016.02.29 (left) and 2016.05.23 (right).

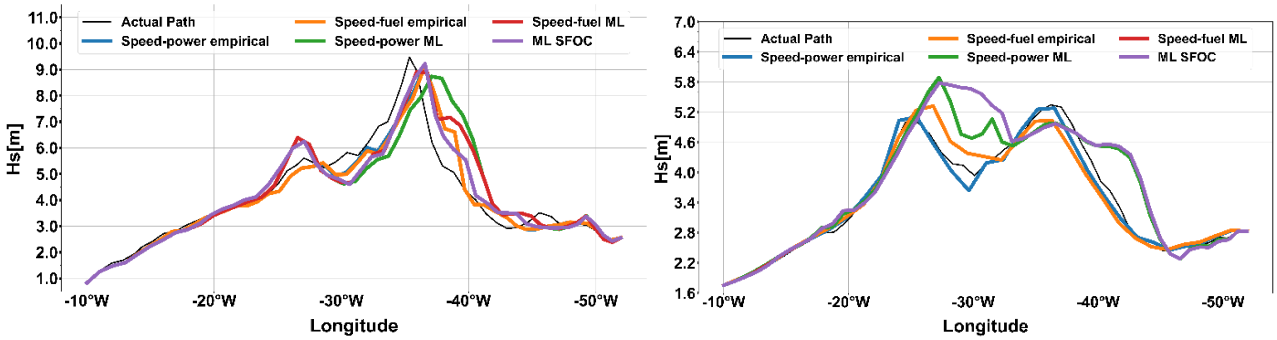

Figure 4.6: Encountered H_s using different energy cost models along Voyage 2016.02.29 (left) and 2016.05.23 (right).

4.2 Summary of Paper II

Various algorithms have been proposed for voyage planning to minimize fuel consumption and increase punctuality, with the isochrone method being recognized for its efficiency. Paper II further enhances the isochrone method to address its limitations in multi-objective optimization and reliable route convergence. Five different improved methods described in Chapter 3.2 are compared to identify the most effective strategy for achieving practicality in real-time applications. The effectiveness

and efficiency of these five improved strategies are compared using data from four ocean-crossing voyages collected by the case study chemical tanker.

To achieve optimal results, the parameters used in the Isochrone optimization algorithm should be well determined, with values listed in Table 4.4. It is found that the parameter Δt can be set to divide the voyage into generally 20 time stages. Following this, $\Delta\theta$, m, ΔD, and r, are chosen based on the actual voyage range and the general sea state. As described in Chapter 3, the local search range for a waypoint is defined by $m \cdot \Delta\theta$, and the entire range of search area is restricted by $r \cdot \Delta D$. $\Delta\theta$ and ΔD indicate the step sizes. For calm sea environments, such as in Voyages 2015.07.21 and 2016.05.23, sailing tends to follow the great circle route to minimize distance. Therefore, the search range can be set smaller. Conversely, for more variable conditions, such as in Voyages 2016.11.08 and 2016.02.29, the values can be set to allow a wider range search.

Table 4.4: Parameters of modified Isochrone algorithm for the full case voyages.

Voyage	$\Delta\theta$ [°]	m	Δt [h]	ΔD	k
Voyage 20161108	0.8	10	8	9	10
Voyage 20150721	0.3	15	7	5	15
Voyage 20160229	0.5	30	8	6	30
Voyage 20160523	0.2	10	8	6	10

Results for westbound voyages

Two westbound voyages, one Voyage 2016.11.08 (winter) and one Voyage 2015.07.21 (summer), are investigated in this section. The optimization results of fuel consumption, sailing time (ETA), and sailing distance are listed in Table 4.5, with the highlighted cells showing the most fuel reductions, and resulting voyages are presented in Figure 4.7.

For Voyage 2015.07.21, all Isochrone-based optimization methods successfully reduced fuel consumption compared to the actual route, achieving savings between 3.9% and 5.7%. In contrast, for Voyage 2016.11.08, certain modified Isochrone methods performed better, notably the Isochrone-A*, Power subsectors, and Isochrone-Dijkstra methods. Specifically, Isochrone-A* demonstrated the best performance with a 2.6% energy improvement. From these two westbound cases, the Isochrone-A* method provided the most energy-efficient route for voyage optimization. The original Isochrone method, however, did not perform well, resulting in the highest fuel consumption, longer sailing distances, and sharp turns near the destination in both cases, as shown in Figure 4.7. Additionally, the Optimal subsectors method behaved similarly to the Reversed subsectors method, with nearly identical routes and comparable fuel expenses in both cases.

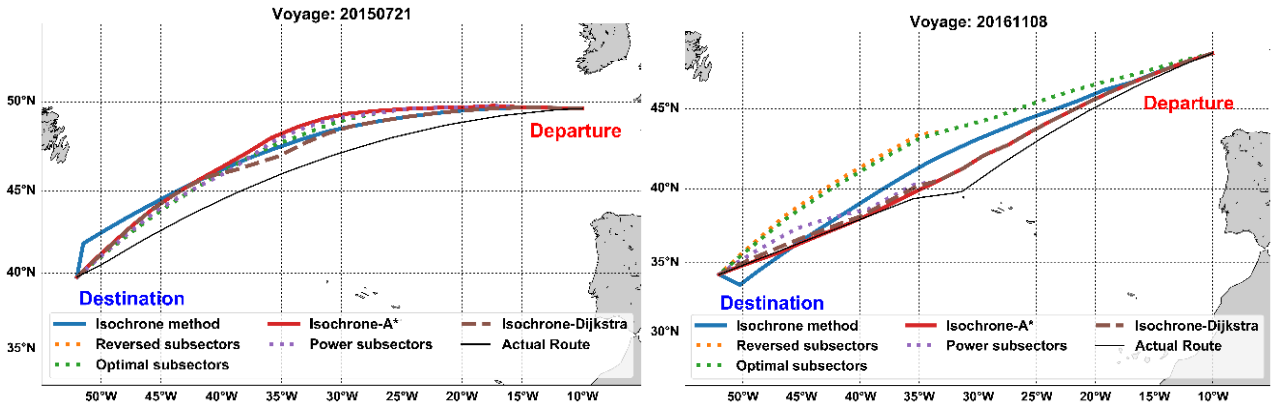

Figure 4.7: Optimization for Voyage 2015.07.21 (left) and 2016.11.08 (right) by different methods.

Table 4.5: Results from the modified Isochrone algorithms for the two westbound voyages.

Optimization Methods	Voyage 2016.11.08				Voyage 2015.07.21			
	ETA [h]	Fuel [ton]	Dis. [km]	Average Speed [knot]	ETA [h]	Fuel [ton]	Dis. [km]	Average Speed [knot]
Actual Route	164.3	159.7	3877.5	12.8	139.8	177.7	3453.6	13.4
Isochrone method	167.8	162.0	3896.1	12.5	142.4	170.8	3533.5	13.4
Reversed subsectors	164.8	163.2	3807.2	12.5	139.8	168.5	3474.3	13.4
Optimal subsectors	164.4	162.9	3798.5	12.5	139.8	168.5	3474.3	13.4
Power subsectors	165.4	156.1	3840.7	12.5	139.9	168.3	3482.3	13.4
Isochrone-A*	165.1	155.6	3836.1	12.5	140.0	167.5	3487.1	13.5
Isochrone-Dijkstra	165.1	155.7	3834.3	12.5	140.0	168.7	3478.0	13.4

Results for eastbound voyages

Two westbound voyages, one Voyage 2016.11.08 in winter and one Voyage 2015.07.21 in summer, are investigated. The optimization results of fuel consumption, sailing time (ETA), and sailing distance are listed in Table 4.6, with the highlighted cells showing the most fuel reductions, and optimized voyages presented in Figure 4.8.

The chosen eastbound voyages encountered challenging sea conditions in the North Atlantic. The winter Voyage 2016.02.29 presents a journey through extremely rough weather, experiencing significant wave heights (*Hs*) of up to 9 meters. To avoid the storm, the actual route first headed slightly south of the GC route before turning back towards the destination. Conversely, the summer Voyage 2016.05.23 faced more typical North Atlantic conditions with *Hs* reaching around 5 meters. Efficient voyage planning in such conditions is crucial, as fuel consumption can vary greatly. All proposed optimization methods showed considerable improvements in these two cases over the actual routes. For the winter Voyage 2016.02.29, Isochrone-A* achieved the highest fuel savings of approximately

9.0%. For the summer Voyage 2016.05.23, all methods resulted in similar fuel consumption, with Isochrone-A* again leading in savings at 3.8%. Notably, only the original Isochrone method resulted in higher fuel consumption than the actual route.

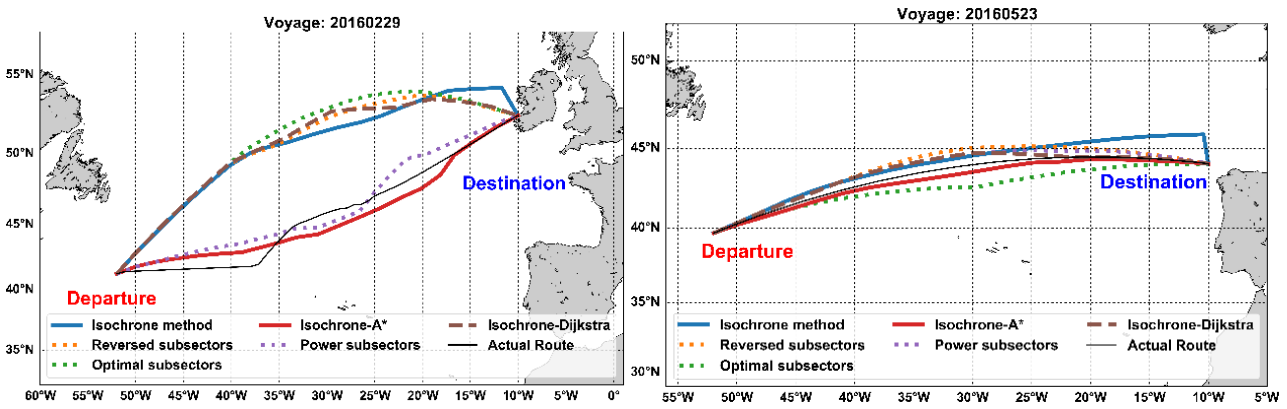

Figure 4.8: Optimization for Voyage 2016.02.29 (left) and 2016.05.23 (right) by different methods.

Table 4.6: Results of the modified Isochrone algorithms for the two eastbound voyages.

Optimization Methods	Voyage 2016.02.29				Voyage 2016.05.23			
	ETA [h]	Fuel [ton]	Dis. [km]	Average Speed [knots]	ETA [h]	Fuel [ton]	Dis. [km]	Average Speed [knots]
Actual Route	159.0	171.5	3624.9	12.3	144.5	156.2	3476.8	13.0
Isochrone method	161.7	164.2	3539.0	11.8	152.3	156.8	3628.8	12.9
Reversed subsectors	159.6	164.6	3450.0	11.7	146.6	151.7	3484.9	12.8
Optimal subsectors	161.4	168.5	3465.6	11.6	146.6	151.1	3491.2	12.9
Power subsectors	159.6	158.9	3549.4	12.0	146.4	151.0	3481.7	12.8
Isochrone-A*	159.9	156.1	3586.5	12.1	145.8	150.2	3479.3	12.9
Isochrone-Dijkstra	159.9	162.6	3453.1	11.7	146.5	151.2	3483.6	12.8

4.3 Summary of Paper III

Based on the measures discussed in Paper I and II, Paper III presents the Isochrone-based Predictive Optimization (IPO) approach, which exhibits improved and resilient performance in real-time, multi-objective voyage optimization. Unlike conventional Isochrone and graph search techniques, this method avoids unrealistic routes with sudden turns. The IPO approach proposes energy-efficient pathways across various sailing conditions while adhering to timeliness requirements. It is computationally efficient, enabling real-time updates and adjustments during the voyage to accommodate changing conditions. The efficiency and effectiveness of the IPO method are demonstrated through the six case study voyages in Figure 4.2 from the chemical tanker in Chapter 4. The results are further

compared with other widely used voyage optimization methods, highlighting the capability of the IPO method in providing energy-efficient and punctual voyage optimization solutions.

4.3.1 Physics-informed ML performance model

The ship model employed in this study is derived from the research conducted by (Lang et al., 2024). As discussed in Paper I, the energy cost function is crucial as they guide decision-making for optimization algorithm. A dependable ship model that accurately forecasts the vessel's performance at sea ensures that the voyage optimization results are trustworthy for practical use.

Otherwise, the optimization could lead to distorted and unreliable results during actual sailing. In Paper III, a state-of-the-art grey-box model (GBM) constructed using a novel physics-informed machine learning approach is employed, which predicts fuel consumption based on the sailing speed of ocean-crossing ships.

A GBM combines the physical principles of WBMs with the data-driven inferences of BBMs, offering higher accuracy, improved interpretability and extrapolation capability. This avoids the unreasonable results sometimes produced by BBMs. In this GBM, a BBM and a physics-informed neural network (PINNs) model are integrated to describe the relationship between the speed over ground (V_g) and the ship's power (P_s). First, the reduction in the ship's speed (ΔV) from V_g is estimated via a BBM, using data related to operations and environmental conditions, and obtaining the speed through water (V) where $V = V_g + \Delta V$. Using V, P_s is predicted through the PINNs model, achieving accurate predictions of engine power needed to achieve the expected speed (V_g). Furthermore, actual variation of *SFOC* is also included to predict more precise fuel costs.

The model assumes the ship is fully loaded with the same draft throughout the voyage. Using a specific speed-fuel model and a reference route, the IPO method can be applied to optimize voyages for various types of ships and trades, extending beyond the chemical tanker originally utilized.

4.3.2 Results of the voyage optimization

In addition to the actual voyages, the four optimization methods detailed in Table 4.7 are also used for comparison with the proposed IPO method. These comparisons highlight the IPO method's practical applicability for real-time voyage optimization across different methods and scenarios.

GC routing is a traditional manual navigation method used in industrial practice. It follows the shortest GC route as a fixed path and divides the route into several time stages based on ETA. The speed of the sub-routes can be adjusted according to local sea conditions to ensure punctuality. It serves as a baseline to verify the practicality of the proposed method for real operations. MI (modified

Isochrone) is where the proposed IPO method derived from, allowing for a comparison to demonstrate IPO's improvements. The 2D Dijkstra algorithm (2DDA) is a widely used method known for its optimization capability and generalization, and the 3D Dijkstra algorithm (3DDA) is an enhanced version of 2DDA that includes speed optimization. They can provide a standard for comparison outside of Isochrone types.

Table 4.7: Four voyage optimization methods used in the comparison.

Method	Description	Reference
GC	Traditional GC routing	-
MI	Modified Isochrone method	(Hagiwara, 1989)
2DDA	Conventional 2D Dijkstra algorithm	(Dijkstra, 1959)
3DDA	3D Dijkstra algorithm	(Wang et al., 2019)

To ensure optimal performance, each method must define a grid. The MI method uses the same parameters as the proposed IPO method for consistency. GC Routing involves testing different speeds within a specified range to accurately meet the ETA, accounting for unintended speed reductions. The number of speed trials is aligned with the number of candidate routes used by the IPO method. Both 2DDA and 3DDA require discretizing the sailing area into a fixed grid, with the grids set to have the same number of time stages as those used in the IPO method.

Results for westbound voyages

In the North Atlantic, storms driven by the prevailing westerlies generally move from west to east, resulting in ships facing more head-on waves on westbound voyages. This makes westbound navigation more challenging and fuel-intensive, necessitating careful planning to improve efficiency and safety. This paper investigates three westbound voyage cases: one in winter and two in summer. The optimization results are summarized in Table 4.8, with ETA, fuel consumption, sailing distance, average speed, and runtime for each voyage. The actual voyage is highlighted in grey, and the proposed method's result is highlighted in green. The optimized routes generated by each method are illustrated in Figure 4.9.

For Voyage 2015.07.21, 2DDA and 3DDA show the least fuel consumption but with 7-hour and 2-hour arrival delays respectively. Considering punctuality, the IPO method achieves the most significant fuel reduction at 7.3%. For Voyage 2016.07.19, IPO and 3DDA closely result in the largest reductions at 3.0% with accurate ETAs. For Voyage 2016.11.08, IPO and 2DDA provide the most fuel savings at around 3.0%, and 2DDA again fails to meet the ETA.

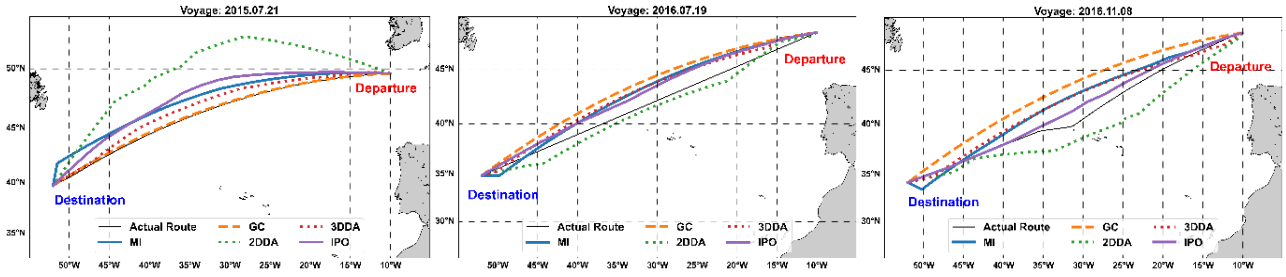

Figure 4.9: Optimized voyages for three westbound cases.

In summary, across the three voyages, IPO consistently delivers the most energy-efficient routes with on-time arrivals. Although IPO and 3DDA result in similar fuel cost, the IPO method operates roughly 90 times faster than 3DDA and twice as fast as 2DDA in terms of runtime. Although 2DDA can offer considerable fuel savings, it frequently fails to guarantee the ETA and often suggests longer sailing routes. GC routing does not demonstrate significant improvements in energy efficiency compared to the actual routes, and the MI method also does not perform well, showing similar fuel consumption to the actual routes with abrupt turns near the destination in all three cases, as depicted in Figure 4.9.

Table 4.8: Result of the three westbound voyages.

Voyage	Category	ETA [h]	Fuel [ton]	Dis. [km]	Ave. Speed [knots/h]	Runtime [s]
2015.07.21	Actual route	139.8	180.6	3453.6	13.3	-
	GC	138.7	180.8	3452.4	13.4	5
	MI	142.4	170.7	3533.5	13.4	25
	2DDA	146.5	161.6	3660.9	13.5	80
	3DDA	142.0	165.9	3462.1	13.2	3432
	IPO	140.0	167.5	3487.1	13.5	40
2016.07.19	Actual route	168.8	141.4	3780.3	12.1	-
	GC	168.5	139.7	3741.8	12.0	4
	MI	168.8	139.5	3783.1	12.1	28
	2DDA	173.4	136.3	3852.4	12.0	76
	3DDA	168.5	137.2	3765.8	12.1	4189
	IPO	168.8	137.4	3749.8	12.0	45
2016.11.08	Actual route	164.3	160.2	3877.5	12.7	-
	GC	163.8	164.1	3789.3	12.5	5
	MI	167.8	162.0	3896.1	12.5	30
	2DDA	172.5	154.2	4024.3	12.6	100
	3DDA	164.0	162.4	3838.4	12.6	4921
	IPO	165.1	155.6	3836.1	12.5	48

Results for eastbound voyages

Eastbound voyages may benefit from the prevailing westerlies, which can boost speed, but the North Atlantic's seasonal variability, particularly rough winter weather, still increases the likelihood of encountering storms. This section details the optimization for one eastbound winter case and two eastbound summer cases, with results shown in Table 4.9. The actual voyage is highlighted in grey, and the proposed method's result is highlighted in green. The optimized routes are illustrated in Figure 4.10.

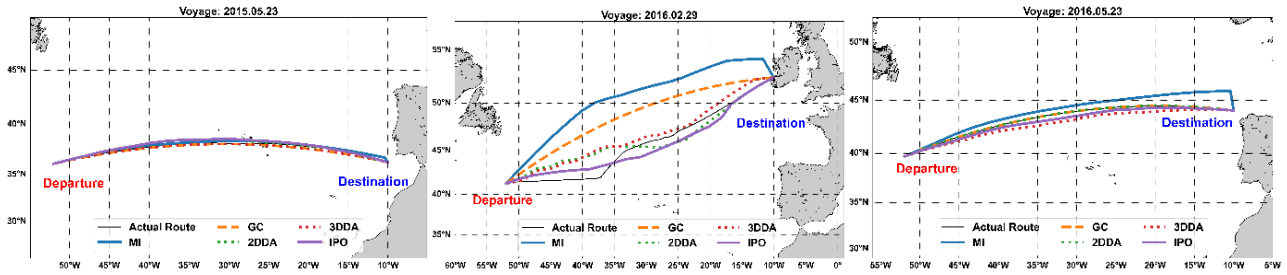

Figure 4.10: Optimized voyages for three eastbound cases.

Table 4.9: Result of the three eastbound voyages.

Voyage	Category	ETA [h]	Fuel [ton]	Dis. [km]	Ave. Speed [knots/h]	Runtime [s]
2015.05.23	Actual route	162.5	139.8	3749.2	12.5	-
	GC	162.4	136.6	3746.6	12.5	4
	MI	162.6	137.6	3764.9	12.5	22
	2DDA	162.6	136.7	3758.7	12.5	70
	3DDA	162.5	136.0	3746.6	12.5	2995
	IPO	162.5	136.0	3749.5	12.5	36
2016.02.29	Actual route	159.0	170.8	3624.9	12.3	-
	GC	159.1	166.8	3374.0	11.5	6
	MI	161.7	164.2	3539.0	11.8	36
	2DDA	161.2	153.2	3589.7	12.0	111
	3DDA	159.0	151.8	3519.6	12.0	6458
	IPO	159.9	156.1	3586.5	12.1	56
2016.05.23	Actual route	144.5	153.7	3476.8	13.0	-
	GC	150.0	155.3	3476.7	13.0	6
	MI	152.2	154.8	3628.8	12.9	24
	2DDA	145.7	150.4	3476.7	12.9	91
	3DDA	144.5	150.8	3482.7	13.0	3660
	IPO	144.8	150.2	3479.3	12.9	41

These voyages face diverse sailing conditions. The winter voyage encounters severe weather, with significant wave heights (H_s) exceeding 9 meters. The summer voyages are calmer, with waves peaking around 5 meters, similar to the westbound voyages. Effective optimization is crucial for such eastbound sailings to prevent inefficiencies that could have serious consequences.

For the winter Voyage 2016.02.29, IPO and 3DDA achieve significant fuel reductions of 8.6% and 11.1%, respectively, while maintaining punctuality. For the summer Voyages 2015.05.23 and 2016.05.23, where sea conditions are relatively moderate, optimization results for each method are relatively close, with IPO and 3DDA achieving the lowest fuel costs at around 3%.

Details of Voyage 2016.02.29 are further shown in Figure 4.11 as it involves a dramatic environmental change. Throughout this voyage, two storms approach the ship's navigation area, as shown by the two peaks in Figure 4.11. The first storm is located near longitude -35°W, and the second near -25°W. The optimized routes diverge to avoid the first storm (Figure 4.10). The MI route deviates north and encounters lower waves during the first storm, while the other routes, including the actual one, head south and face higher impacts. However, in the second storm, the other routes effectively bypass the storm's main impact, maintaining lower engine power (shown in Figure 4.11). Still, MI requires higher power to avoid the first storm and during the second storm, eventually turning significantly towards the destination to compensate for the detour, resulting in impracticality and time delays.

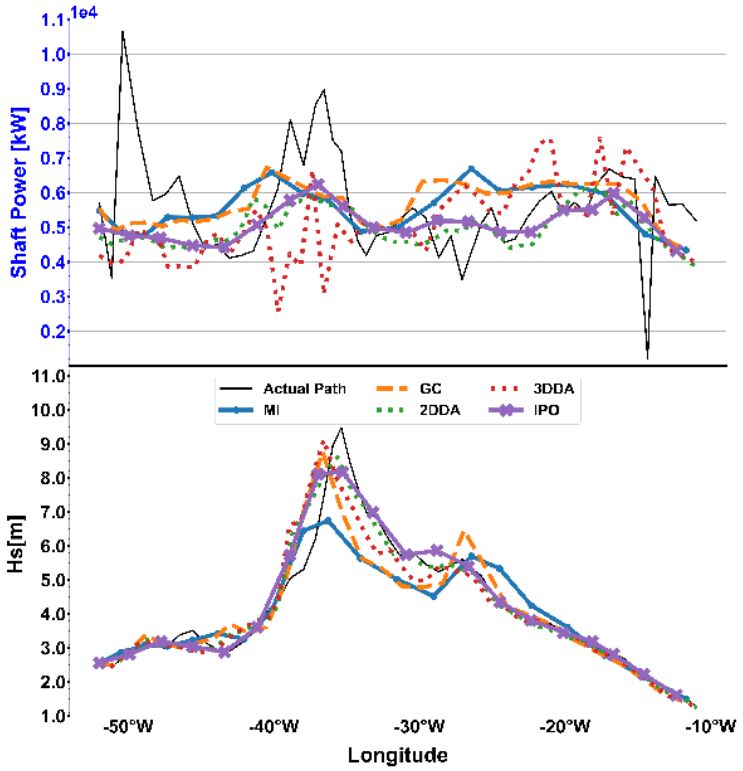

Figure 4.11: Propulsion power and encountered H_s during Voyage 2016.02.29.

Figure 4.12 illustrates the dynamic progression of encountering the second storm. The storm appears to the south, ahead of the four routes that initially head south, and then moves northward and

intensifies, coinciding with MI and GC routes. IPO, 2DDA, 3DDA, and the actual route narrowly miss the storm's center, making MI and GC less efficient. The maneuvers required by the actual route led to increased distance and speed, significantly affected by the first storm. Despite attempts to avoid both storms, this route does not achieve fuel savings given by 3DDA and IPO.

Overall, IPO demonstrates improved performance compared to MI, and shows the best optimization capability among the 2D methods, comparable to 3DDA. Computational efficiency varies, especially for Voyage 2016.02.29, which involves dramatic weather changes and requires a denser grid for a wider search space, increasing the computational load. Despite this, IPO is generally 80 to 100 times faster than 3DDA and twice as fast as 2DDA.

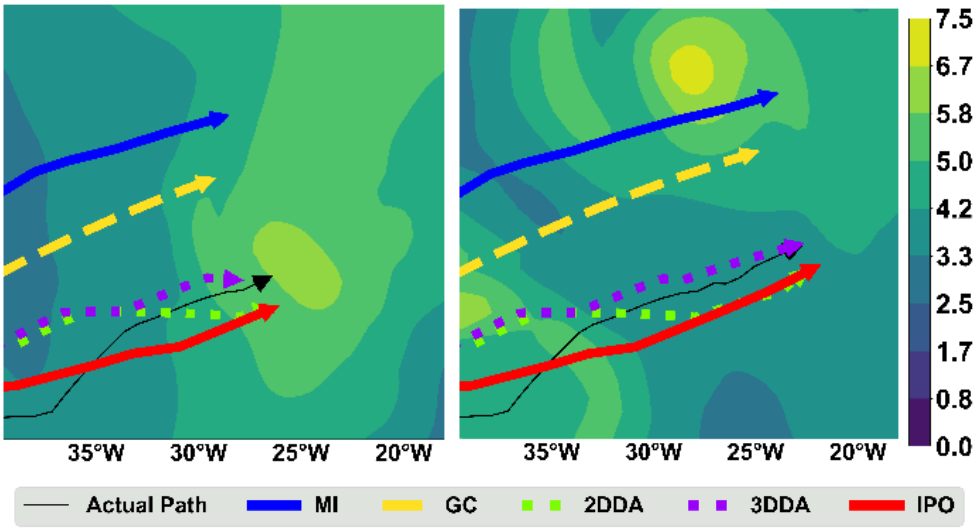

Figure 4.12: Voyage evolution with *Hs* during Voyage 2016.02.29.

5 Conclusions

The development and implementation of voyage optimization systems are essential for the future of autonomous shipping, aligning with both the academia's and industry's goals of sustainability and energy efficiency. This thesis addresses the critical issue of energy-efficient real-time voyage optimization, by proposing an effective and efficient Isochrone-based optimization algorithm. To achieve this objective, three stepwise goals were formulated: 1) Identify the sensitivity of voyage optimizations to different ship performance models, and determine the reliable ship model to be used in voyage optimization. 2) Propose several strategies to improve the Isochrone method for energy efficient real-time voyage optimization, and investigate the most effective strategy. 3) Combing the above findings, propose the Isochrone-based algorithm that addresses voyage optimization problem to optimize energy efficiency and ensure an accurate ETA for the given voyage under diverse sailing conditions. The optimized routes should be smooth for operation, and computation is efficient with runtime within 1 minute, allowing for both voyage planning and real-time execution usage.

Sensitivity of voyage optimizations to different ship performance models

To achieve this goal, Paper I appended in the thesis first investigates the sensitivity of optimization algorithm to various ship energy cost models. It is found that, firstly, voyage optimization is very sensitive to ship models, with differences in energy cost savings reaching up to 10%. Secondly, ML ship models behave stably across different sailing conditions, while theoretical ship models lead to more varied optimization results. Harsher sea conditions with more environmental changes can exacerbate these deviations. Finally, including actual variations of *SFOC* through using a GBM also impacts optimization performance, with 6% to 8% differences in energy cost savings. Thus, it can be concluded that, voyage optimization is very sensitive to ship models; and a GBM, which utilizes ML techniques while considering the actual *SFOC* variation could be a reliable model for voyage optimization.

Strategies to improve the Isochrone method

In Paper II, a traditional voyage optimization method, Isochrone algorithm, is improved as its computational efficiency has been demonstrated by industrial practice. Five strategies are proposed to address the drawbacks of the Isochrone method, specifically, i) resolve the occurrence of irregular routes, ii) improve optimization capability to avoid local optimization, iii) remain computational efficient, which is within 1 minute. The results are compared using case study voyages of a chemical tanker with full-scale measurements. It is found that, all five improvement strategies can lead to an improved capability in energy-efficient voyage optimization compared to the Isochrone method. Among these, one strategy, named Isochrone-A*, is the most effective solution. It can provide smooth

operational routes while also suggesting the most fuel-efficient voyages, offering average fuel savings of 4% to 5% and ensuring on-time arrival. Additionally, it maintains computational efficiency, with a runtime of under 1 minute.

Propose the Isochrone-based algorithm for energy efficient real-time voyage optimization

In Paper III, based on both findings from Paper I and Paper II, an Isochrone-based predictive optimization (IPO) algorithm is proposed for energy efficient ship voyage planning and execution. Firstly, a state-of-the-art ship performance GBM which considers actual *SFOC* effects, is used to provide reliable performance predictions under diverse sea states. Secondly, based on Isochrone A* strategy, two improvements are introduced to enhance the Isochrone method: the waypoint grid is refined to smooth the route, and predictive optimization is further introduced by refining the cost function to avoid local optima. Its performance is validated through six case study voyages of a chemical tanker, and also compared with four established voyage optimization techniques using full-scale data. The analysis demonstrates that the IPO method provides smoother voyages with more gradual turns, resulting in an average reduction of 5% in fuel consumption across all voyage cases, and with a runtime of approximately 40 seconds, making real-time adjustment to dynamic sailing conditions possible. Other voyage optimizations techniques included for comparison, either show no fuel savings or less than 5%, or their computational time is at least 2 times longer.

6 Future work

The research focuses on developing real-time voyage optimization algorithms to support autonomous and intelligent navigation. The current work primarily addresses the real-time voyage optimization problem for seagoing vessels in open sea sailing conditions, considering their transportation needs such as energy efficiency and on-time arrivals. However, based on assumptions and limitations discussed in Chapter 1.3, there are other challenges that need investigations.

Collision avoidance in short sea shipping

Real-time autonomous navigation is crucial not only for ocean-crossing shipping but also for coastal and short sea shipping. Specifically, because of the more dynamic environmental changes such as varying terrains and traffic conditions, the real-time capability is even more significant and valuable for short sea shipping navigation.

As the research has proposed the IPO, which has demonstrated real-time and adaptive capabilities, the IPO method also shows potential and possibility to be applied in short sea navigation and voyage optimization. In such scenarios, voyage execution becomes even more challenging, therefore can benefit greatly from real-time voyage optimizations.

However, implementation scenarios change in short sea navigation, thereby altering objectives and constraints accordingly. For example, waypoint generation needs to consider terrains, which restricts the feasible search area. Operational safety becomes the top priority because of increased interactions between other ships, making collision-free voyages essential. Since substantial traffic flows involving numerous ships could occur, collision avoidance must comply with international regulations such as the well-known International Regulations for Preventing Collisions at Sea (COLREGs) published by the IMO (IMO, 1972), or other reginal waterway regulations defined by local authorities, such as the Netherlands' inland navigation police regulations (BPR, 2017) and Central commission for the navigation of the Rhine (CCNR, 2023) for Rhine River.

In addition to regulation compliance, evaluating the collision risk with other ships is necessary to achieve the safest route. Thus, ship domain and safety models are also needed. Furthermore, energy efficiency and on-time arrivals remain important objectives. Therefore, optimization in short sea shipping requires specific considerations such as land-crossing and shallow water avoidance, collision avoidance, traffic regulations compliance, and collision risk assessment based on ship domain and ship safety models, etc. This comprehensive approach could effectively address the unique challenges of short sea navigation.

Investigate the effectiveness of using ML techniques in real-time collision avoidance navigation

As more components are integrated into a comprehensive navigation system for applications, optimization challenges can escalate in scale and complexity. The algorithm's strengths in areas like big data classification, online execution, and dynamic adaptive optimization will prove advantageous. Consequently, deploying advanced optimization algorithms could also yield superior optimization outcomes and achieve rapid computational speeds in such scenarios. Notably, the application of advanced techniques such as hybrid heuristics (Atyabi & Powers, 2013), metaheuristics (Singh et al., 2022), and hyper-heuristics (Singh & Pillay, 2022), along with adaptive(Chen & Tan, 2023), self-adaptive, and machine learning algorithms, has shown promising results in fields including transportation (Dulebenets, 2021), online scheduling (Dulebenets, 2021), and multi-objective optimization (Sekkal & Belkaid, 2023). Future research can also explore their potential in the complex and challenging collision avoidance voyage optimization, or consider their integration into the proposed method to enhance its performance in short sea and inland shipping.

Integrate ship models in confined waterways

The cost function also needs to include ship models which are adapted to suit short sea and coastal shipping. Compared to seagoing vessels, these ship models must account for specific effects, e.g., the bank effect or maneuverability in areas close to shore, etc. Additionally, the cost function can also include evaluation of the energy cost for short sea and coastal sailings. This tailors the cost function to the unique conditions of short sea navigation to provide accurate and efficient voyage optimization. The study of ship models for inland and coastal shipping is also a popular field with ongoing research. Due to the various unique conditions that differ from those in open sea environments, they need to be specifically considered in inland and coastal shipping models. Therefore, similar to research conducted for open sea sailing in this thesis, it can also be important to investigate which types of models are effective for optimization in these contexts.

Real case study and validation

The behavior of traffic ships can be unpredictable with constantly changing trajectories, as their future movements may not be strongly correlated with their previous ones, due to varying operational tasks and conditions. Therefore, simulations may not fully capture the complexity of real traffic situations. Consequently, validating the algorithm based on real traffic data is necessary to demonstrate its effectiveness, especially for voyage execution phase.

References

Ahlgren, F., Mondejar, M. E., & Thern, M. (2019). Predicting dynamic fuel oil consumption on ships with automated machine learning. *Energy Procedia*, *158*, 6126-6131.

Ari, I., Aksakalli, V., Aydogdu, V., & Kum, S. (2013). Optimal ship navigation with safety distance and realistic turn constraints. *European Journal of Operational Research*, *229*(3), 707-717.

Atyabi, A., & Powers, D. (2013). Review of classical and heuristic-based navigation and path planning approaches. *International Journal of Advancements in Computing Technology (IJACT)*, *5*(14).

Bahrami, N., & Siadatmousavi, S. M. (2023). Ship voyage optimisation considering environmental forces using the iterative Dijkstra's algorithm. *Ships and Offshore Structures*, 1-8.

Bai, X., Cheng, L., & Iris, Ç. (2022). Data-driven financial and operational risk management: Empirical evidence from the global tramp shipping industry. *Transportation Research Part E: Logistics and Transportation Review*, *158*, 102617.

Bassam, A. M., Phillips, A. B., Turnock, S. R., & Wilson, P. A. (2023). Artificial neural network based prediction of ship speed under operating conditions for operational optimization. *Ocean Engineering*, *278*, 114613.

Bellman, R. (1952). On the theory of dynamic programming. *Proceedings of the national Academy of Sciences*, *38*(8), 716-719.

Beşikçi, E. B., Arslan, O., Turan, O., & Ölçer, A. I. (2016). An artificial neural network based decision support system for energy efficient ship operations. *Computers & Operations Research*, *66*, 393-401.

BPR. (2017). *Binnenvaartpolitiereglement*. Retrieved August 21st from https://wetten.overheid.nl/BWBR0003628/2017-01-01#DeelI

CCNR. (2023). *Central Commission for the Navigation of the Rhine - CCNR Regulations*. Retrieved August 21st from https://www.ccr-zkr.org/13020500-en.html

Chen, M., & Tan, Y. (2023). SF-FWA: A Self-Adaptive Fast Fireworks Algorithm for effective large-scale optimization. *Swarm and Evolutionary Computation*, *80*, 101314.

Chen, T., & Guestrin, C. (2016). Xgboost: A scalable tree boosting system. Proceedings of the 22nd acm sigkdd international conference on knowledge discovery and data mining,

Choi, G.-H., Lee, W., & Kim, T.-w. (2023). Voyage optimization using dynamic programming with initial quadtree based route. *Journal of Computational Design and Engineering*, *10*(3), 1185-1203.

Christiansen, M., Fagerholt, K., Nygreen, B., & Ronen, D. (2007). Maritime transportation. *Handbooks in operations research and management science*, *14*, 189-284.

Coraddu, A., Oneto, L., Baldi, F., & Anguita, D. (2017). Vessels fuel consumption forecast and trim optimisation: A data analytics perspective. *Ocean Engineering*, *130*, 351-370.

De Wit, C. (1990). Proposal for low cost ocean weather routeing. *The Journal of Navigation*, *43*(3), 428-439.

Dijkstra, E. W. (1959). A note on two problems in connexion with graphs [Article]. *Numerische Mathematik*, *1*(1), 269-271. https://doi.org/10.1007/BF01386390

Dong, L., Li, J., Xia, W., & Yuan, Q. (2021). Double ant colony algorithm based on dynamic feedback for energy-saving route planning for ships. *Soft Computing*, *25*, 5021-5035.

Du, W., Li, Y., Zhang, G., Wang, C., Zhu, B., & Qiao, J. (2022). Energy saving method for ship weather routing optimization. *Ocean Engineering*, *258*, 111771.

Du, Y., Meng, Q., Wang, S., & Kuang, H. (2019). Two-phase optimal solutions for ship speed and trim optimization over a voyage using voyage report data. *Transportation Research Part B: Methodological*, *122*, 88-114.

Dulebenets, M. A. (2021). An Adaptive Polyploid Memetic Algorithm for scheduling trucks at a cross-docking terminal. *Information Sciences*, *565*, 390-421.

European Centre for Medium-Range Weather Forecasts. *European Centre for Medium-Range Weather Forecasts (ECMWF)*. https://www.ecmwf.int/

Regulation (EU) 2015/757 of the European Parliament and of the Council, August 21st (2015). https://eur-lex.europa.eu/eli/reg/2015/757/oj

Fan, A., Yang, J., Yang, L., Wu, D., & Vladimir, N. (2022). A review of ship fuel consumption models. *Ocean Engineering*, *264*, 112405.

Fang, M.-C., & Lin, Y.-H. (2015). The optimization of ship weather-routing algorithm based on the composite influence of multi-dynamic elements (II): Optimized routings. *Applied Ocean Research*, *50*, 130-140.

Gao, Y., & Sun, Z. (2023). Tramp ship routing and speed optimization with tidal berth time windows. *Transportation Research Part E: Logistics and Transportation Review*, *178*, 103268.

Gasparetto, A., Boscariol, P., Lanzutti, A., & Vidoni, R. (2015). Path planning and trajectory planning algorithms: A general overview. *Motion and operation planning of robotic systems: Background and practical approaches*, 3-27.

Gkerekos, C., & Lazakis, I. (2020). A novel, data-driven heuristic framework for vessel weather routing. *Ocean Engineering*, *197*, 106887.

Hagiwara, H. (1989). Weather routing of (sail-assisted) motor vessels. *Ph. D. thesis, Delft Univ. Tech.*

Hart, P. E., Nilsson, N. J., & Raphael, B. (1968). A formal basis for the heuristic determination of minimum cost paths. *IEEE transactions on Systems Science and Cybernetics*, *4*(2), 100-107.

Holtrop, J., & Mennen, G. (1982). An approximate power prediction method. *International Shipbuilding Progress*, *29*(335), 166-170.

Huang, L., Wen, Y., Geng, X., Zhou, C., & Xiao, C. (2018). Integrating multi-source maritime information to estimate ship exhaust emissions under wind, wave and current conditions. *Transportation Research Part D: Transport and Environment*, *59*, 148-159.

IMO. (1972). *Convention on the International Regulations for Preventing Collisions at Sea, 1972 (COLREGs)*. Retrieved August 21st from https://www.imo.org/en/About/Conventions/Pages/COLREG.aspx

IMO. (1999). *Guidelines for Voyage Planning (Resolution A.893(21))* (A.893(21)). International Maritime Organization. https://wwwcdn.imo.org/localresources/en/KnowledgeCentre/IndexofIMOResolutions/AssemblyDocuments/A.893(21).pdf

IMO. (2003). *Guidance note on the preparation of proposals on ships' routeing systems and ship reporting systems for submission to the sub-committee on safety of navigation*. https://wwwcdn.imo.org/localresources/en/OurWork/Safety/Documents/Ships%27%20routeing/MSC.1-Circ.1060-asAmended-consolidated-Guidance%20Note%20on%20the%20Preparation%20of%20Proposals%20onShipsRouteingReporting.pdf

IMO. (2020a). *Fourth IMO Greenhouse Gas Study 2020*. I. M. Organization. https://wwwcdn.imo.org/localresources/en/OurWork/Environment/Documents/Fourth%20IMO%20GHG%20Study%202020%20-%20Full%20report%20and%20annexes.pdf

IMO. (2020b). *Just In Time Arrival Guide: Barriers and Potential Solutions*. International Maritime Organization. https://greenvoyage2050.imo.org/wp-content/uploads/2021/01/GIA-just-in-time-hires.pdf

James, R. (1957). Application of wave forecast to marine navigation. Washington.

Jeong, S., Jeong, D., Park, J., Kim, S., & Kim, B. (2019). A voyage optimization model of LNG carriers considering boil-off gas. OCEANS 2019 MTS/IEEE SEATTLE,

Klompstra, M. B., Olsder, G., & Van Brunschot, P. (1992). The isopone method in optimal control. *Dynamics and Control*, *2*(3), 281-301.

Lang, X., & Mao, W. (2020). A semi-empirical model for ship speed loss prediction at head sea and its validation by full-scale measurements. *Ocean Engineering*, *209*, 107494.

Lang, X., & Mao, W. (2021). A practical speed loss prediction model at arbitrary wave heading for ship voyage optimization. *Journal of Marine Science and Application*, *20*(3), 410-425.
Lang, X., Wu, D., & Mao, W. (2021). Benchmark Study of Supervised Machine Learning Methods for a Ship Speed-Power Prediction at Sea. International Conference on Offshore Mechanics and Arctic Engineering,
Lang, X., Wu, D., & Mao, W. (2022). Comparison of supervised machine learning methods to predict ship propulsion power at sea. *Ocean Engineering*, *245*, 110387.
Lang, X., Wu, D., & Mao, W. (2024). Physics-informed machine learning models for ship speed prediction. *Expert Systems with Applications*, *238*, 121877.
Lee, S.-J., Sun, Q., & Meng, Q. (2023). Vessel weather routing subject to sulfur emission regulation. *Transportation Research Part E: Logistics and Transportation Review*, *177*, 103235.
Li, P.-F., Wang, H.-B., & He, D.-Q. (2018). Ship weather routing based on improved ant colony optimization algorithm. 2018 IEEE Industrial Cyber-Physical Systems (ICPS),
Li, X., Sun, B., Guo, C., Du, W., & Li, Y. (2020). Speed optimization of a container ship on a given route considering voluntary speed loss and emissions. *Applied Ocean Research*, *94*, 101995.
Lin, Y.-H. (2018). The simulation of east-bound transoceanic voyages according to ocean-current sailing based on Particle Swarm Optimization in the weather routing system. *Marine Structures*, *59*, 219-236.
Lin, Y.-H., Fang, M.-C., & Yeung, R. W. (2013). The optimization of ship weather-routing algorithm based on the composite influence of multi-dynamic elements. *Applied Ocean Research*, *43*, 184-194.
Ma, D., Zhou, S., Han, Y., Ma, W., & Huang, H. (2024). Multi-objective ship weather routing method based on the improved NSGA-III algorithm. *Journal of Industrial Information Integration*, *38*, 100570.
Ma, W., Lu, T., Ma, D., Wang, D., & Qu, F. (2021). Ship route and speed multi-objective optimization considering weather conditions and emission control area regulations. *Maritime Policy & Management*, *48*(8), 1053-1068.
Majumder, A., & Majumder, A. (2021). Pathfinding and navigation. *Deep Reinforcement Learning in Unity: With Unity ML Toolkit*, 73-153.
Mannarini, G., & Carelli, L. (2019). VISIR-1. b: Ocean surface gravity waves and currents for energy-efficient navigation. *Geoscientific Model Development*, *12*(8), 3449-3480.
Mannarini, G., Salinas, M. L., Carelli, L., Petacco, N., & Orović, J. (2023). VISIR-2: ship weather routing in Python. *EGUsphere*, *2023*, 1-40.
Mao, W., Ringsberg, J. W., Rychlik, I., & Li, Z. (2012). Theoretical development and validation of a fatigue model for ship routing. *Ships and Offshore Structures*, *7*(4), 399-415.
Mao, W., & Rychlik, I. (2017). Estimation of Weibull distribution for wind speeds along ship routes. *Proceedings of the Institution of Mechanical Engineers, Part M: Journal of Engineering for the Maritime Environment*, *231*(2), 464-480.
Moradi, M. H., Brutsche, M., Wenig, M., Wagner, U., & Koch, T. (2022). Marine route optimization using reinforcement learning approach to reduce fuel consumption and consequently minimize CO2 emissions. *Ocean Engineering*, *259*, 111882.
Poulsen, R. T., Viktorelius, M., Varvne, H., Rasmussen, H. B., & von Knorring, H. (2022). Energy efficiency in ship operations-Exploring voyage decisions and decision-makers. *Transportation Research Part D: Transport and Environment*, *102*, 103120.
Roh, M.-I. (2013). Determination of an economical shipping route considering the effects of sea state for lower fuel consumption. *International Journal of Naval Architecture and Ocean Engineering*, *5*(2), 246-262.
Sekkal, D. N., & Belkaid, F. (2023). A multi-objective optimization algorithm for flow shop group scheduling problem with sequence dependent setup time and worker learning. *Expert Systems with Applications*, *233*, 120878.

Shin, Y. W., Abebe, M., Noh, Y., Lee, S., Lee, I., Kim, D., Bae, J., & Kim, K. C. (2020). Near-optimal weather routing by using improved A* algorithm. *Applied Sciences*, *10*(17), 6010.

Ships, I. (2015). marine technology—Guidelines for the assessment of speed and power performance by analysis of speed trial data. *ISO: Geneva, Switzerland*.

Simonsen, M. H., Larsson, E., Mao, W., & Ringsberg, J. W. (2015). State-of-the-art within ship weather routing. International Conference on Offshore Mechanics and Arctic Engineering,

Singh, E., & Pillay, N. (2022). A study of ant-based pheromone spaces for generation constructive hyper-heuristics. *Swarm and Evolutionary Computation*, *72*, 101095.

Singh, P., Pasha, J., Moses, R., Sobanjo, J., Ozguven, E. E., & Dulebenets, M. A. (2022). Development of exact and heuristic optimization methods for safety improvement projects at level crossings under conflicting objectives. *Reliability Engineering & System Safety*, *220*, 108296.

Soner, O., Akyuz, E., & Celik, M. (2018). Use of tree based methods in ship performance monitoring under operating conditions. *Ocean Engineering*, *166*, 302-310.

Stevenson, A. (2010). *Oxford Dictionary of English*. Oxford University Press.

Szlapczynska, J., & Szlapczynski, R. (2019). Preference-based evolutionary multi-objective optimization in ship weather routing. *Applied Soft Computing*, *84*, 105742.

Tillig, F., & Ringsberg, J. W. (2019). A 4 DOF simulation model developed for fuel consumption prediction of ships at sea. *Ships and Offshore Structures*, *14*(sup1), 112-120.

Tsou, M.-C. (2010). Integration of a geographic information system and evolutionary computation for automatic routing in coastal navigation. *The Journal of Navigation*, *63*(2), 323-341.

Tzortzis, G., & Sakalis, G. (2021). A dynamic ship speed optimization method with time horizon segmentation. *Ocean Engineering*, *226*, 108840.

UNCTAD. (2021). *Review of Maritime Transport 2021 (UNCTAD/RMT/2021)*. United Nations Publication. Retrieved August from https://unctad.org/system/files/official-document/rmt2021_en_0.pdf

Vettor, R., Bergamini, G., & Guedes Soares, C. (2021). A comprehensive approach to account for weather uncertainties in ship route optimization. *Journal of Marine Science and Engineering*, *9*(12), 1434.

Wang, H., Lang, X., & Mao, W. (2021). Voyage optimization combining genetic algorithm and dynamic programming for fuel/emissions reduction. *Transportation Research Part D: Transport and Environment*, *90*, 102670.

Wang, H., Mao, W., & Eriksson, L. (2019). A Three-Dimensional Dijkstra's algorithm for multi-objective ship voyage optimization. *Ocean Engineering*, *186*, 106131.

Wang, H., Yan, R., Wang, S., & Zhen, L. (2023). Innovative approaches to addressing the tradeoff between interpretability and accuracy in ship fuel consumption prediction. *Transportation Research Part C: Emerging Technologies*, *157*, 104361.

Wang, K., Guo, X., Zhao, J., Ma, R., Huang, L., Tian, F., Dong, S., Zhang, P., Liu, C., & Wang, Z. (2022). An integrated collaborative decision-making method for optimizing energy consumption of sail-assisted ships towards low-carbon shipping. *Ocean Engineering*, *266*, 112810.

Wang, K., Li, J., Huang, L., Ma, R., Jiang, X., Yuan, Y., Mwero, N. A., Negenborn, R. R., Sun, P., & Yan, X. (2020). A novel method for joint optimization of the sailing route and speed considering multiple environmental factors for more energy efficient shipping. *Ocean Engineering*, *216*, 107591.

Wen, S., Jin, X., Zheng, Y., & Wang, M. (2023). Probabilistic coordination of optimal power management and voyage scheduling for all-electric ships. *IEEE Transactions on Transportation Electrification*.

Wisniewski, B. (1991). Methods of route selection for a sea going vessel. *Gdansk: Wydawnictwo Morskie*.

Wu, L., Wang, S., & Laporte, G. (2021). The robust bulk ship routing problem with batched cargo selection. *Transportation Research Part B: Methodological*, *143*, 124-159.
Xue, H. (2022). A quasi-reflection based SC-PSO for ship path planning with grounding avoidance. *Ocean Engineering*, *247*, 110772.
Yan, R., Wang, S., & Du, Y. (2020). Development of a two-stage ship fuel consumption prediction and reduction model for a dry bulk ship. *Transportation Research Part E: Logistics and Transportation Review*, *138*, 101930.
Yan, R., Wu, S., Jin, Y., Cao, J., & Wang, S. (2022). Efficient and explainable ship selection planning in port state control. *Transportation Research Part C: Emerging Technologies*, *145*, 103924.
Yan, R., Yang, D., Wang, T., Mo, H., & Wang, S. (2024). Improving ship energy efficiency: Models, methods, and applications. *Applied Energy*, *368*, 123132.
Yang, L., Chen, G., Rytter, N. G. M., Zhao, J., & Yang, D. (2019). A genetic algorithm-based grey-box model for ship fuel consumption prediction towards sustainable shipping. *Annals of Operations Research*, 1-27.
Yu, H., Fang, Z., Fu, X., Liu, J., & Chen, J. (2021). Literature review on emission control-based ship voyage optimization. *Transportation Research Part D: Transport and Environment*, *93*, 102768.
Yuan, Q., Wang, S., Zhao, J., Hsieh, T.-H., Sun, Z., & Liu, B. (2022). Uncertainty-informed ship voyage optimization approach for exploiting safety, energy saving and low carbon routes. *Ocean Engineering*, *266*, 112887.
Zaccone, R., Ottaviani, E., Figari, M., & Altosole, M. (2018). Ship voyage optimization for safe and energy-efficient navigation: A dynamic programming approach. *Ocean Engineering*, *153*, 215-224.
Zhang, C., Zhang, D., Zhang, M., Zhang, J., & Mao, W. (2022). A three-dimensional ant colony algorithm for multi-objective ice routing of a ship in the Arctic area. *Ocean Engineering*, *266*, 113241.
Zhang, M., Ren, H., & Zhou, Y. (2023). Research on global ship path planning method based on improved ant colony algorithm. *IEEE Open Journal of Intelligent Transportation Systems*, *4*, 143-152.
Zhao, Y., Zhou, J., Fan, Y., & Kuang, H. (2019). An expected utility-based optimization of slow steaming in sulphur emission control areas by applying big data analytics. *Ieee Access*, *8*, 3646-3655.
Zhen, L., Hu, Z., Yan, R., Zhuge, D., & Wang, S. (2020). Route and speed optimization for liner ships under emission control policies. *Transportation Research Part C: Emerging Technologies*, *110*, 330-345.
Zis, T. P., Psaraftis, H. N., & Ding, L. (2020). Ship weather routing: A taxonomy and survey. *Ocean Engineering*, *213*, 107697.
Życzkowski, M., Krata, P., & Szłapczyński, R. (2018). Multi-objective weather routing of sailboats considering wave resistance. *Polish Maritime Research*, *25*(1), 4-12.
Zyczkowski, M., & Szlapczynski, R. (2023). Collision risk-informed weather routing for sailboats. *Reliability Engineering & System Safety*, *232*, 109015.